Optimal Sizing of Hybrid Renewable Energy Based Microgrid System

by

Irfan Rahman

180021305

Farheen Suha

180021315

Md. Tamim Hasan

180021317

An Undergraduate Thesis submitted to *Islamic University of Technology (IUT)*
in partial fulfillment for the award of the degree of,

Bachelor of Science in Electrical and Electronic Engineering

Department of Electrical and Electronic Engineering (EEE)

Islamic University of Technology (IUT)

Gazipur, Bangladesh

June 2023

CERTIFICATE OF APPROVAL

The thesis titled 'Optimal Sizing of Hybrid Energy Based Microgrid System, submitted by Irfan Rahman (St. Id. 180021305), Farheen Suha (St. Id. 180021315) and Md. Tamim Hasan (St. Id. 180021317) of Academic Year 2020-21 has been found as satisfactory and accepted as partial fulfillment of the requirement for the Degree of BACHELOR OF SCIENCE IN ELECTRICAL AND ELECTRONIC ENGINEERING on June 9, 2023.

Approved By,

____

Dr. Ashik Ahmed
Supervisor and Professor,
Electrical and Electronic Engineering Department,
Islamic University of Technology (IUT)
Board Bazar, Gazipur-1704.
Date: 9^{th} June 2023

DECLARATION OF CANDIDATES

It is hereby declared that this thesis or any part of it has not been submitted elsewhere for award of any degree or diploma.

(Signature of the Candidate)

Irfan Rahman

Student ID: 180021305

(Signature of the Candidate)

Farheen Suha

Student ID: 180021315

(Signature of the Candidate)

Md. Tamim Hasan

Student ID: 180021317

ACKNOWLEDGEMENTS

First and foremost, we offer gratitude to the Almighty Allah (SWT) for giving us the capability to do this work with good health.

We are grateful for the support and advice we have received from our Research Supervisor, Professor Dr. Ashik Ahmed Sir, throughout this work. He created a research environment that made it possible for us to explore many ideas without constraint. With his guidance, we have acquired a lot of knowledge and experience in science and engineering that will be invaluable to our future pursuits.

We would like to thank all the faculty members of the department of EEE, IUT for their inspiration and help.

And last but not the least we are thankful to our family, friends and well-wishers for their support and inspiration. Without them it would never have been possible for us to make it this far.

Thankfully,

Irfan Rahman, 180021305

Farheen Suha, 180021315

Md. Tamim Hasan, 180021317

ABSTRACT

With the decline of fossil fuel reserves and the escalating global average temperature, the quest for environmentally friendly and renewable energy sources has gained significant momentum. Recent interest has focused on wind and photovoltaic and biogas-based energy conversion processes. However, due to the unpredictable nature of their inputs, incorporating energy storage devices is essential to ensure uninterrupted power supply. Furthermore, for hybrid renewable power generation to be economically viable, careful optimization of the participating generating units is imperative.

This thesis presents an optimal sizing approach for a Wind-Photovoltaic-Biogas-Battery system using a single objective optimization (SOO) method. The study compares the performance of seven metaheuristic optimizers: Particle Swarm Optimization (PSO), Aquila Optimizer (AO), Pelican Optimization Algorithm (POA), Dandelion Optimizing Algorithm (DOA), Gazelle Optimization Algorithm (GOA), Zebra Optimization Algorithm (ZOA), and Osprey Optimization Algorithm (OOA).

A comprehensive comparative analysis is conducted, evaluating the convergence speed and objective mean (for minimization) of the applied metaheuristic algorithms. The results demonstrate that the Pelican Optimization Algorithm (POA) outperforms other existing algorithms, exhibiting faster convergence and lower objective mean. These findings highlight the efficacy of POA for optimizing the sizing of hybrid renewable energy systems.

This research contributes to advancing renewable energy systems by addressing intermittent input challenges and facilitating the design optimization of hybrid systems. The findings can serve as valuable insights for energy scientists,

engineers, and policymakers, enabling them to make well-informed choices regarding the deployment and functioning of hybrid renewable energy systems. This will contribute to the promotion of a sustainable and resilient energy landscape, supporting a future that prioritizes environmental sustainability and adaptability.

TABLE OF CONTENTS

LIST OF TABLES

LIST OF FIGURES

List of symbols and abbreviations

a	Constant
b	Constant
α	Power law exponent
β	Tilt angle in degree
δ	Declination
η_{bat}	Efficiency of battery
ω	Solar hour angle
φ	Latitude of a site
ρ_g	Ground reflectance
σ	Self -discharge rate of battery
η_b	Battery charging efficiency
η_{PV}	Efficiency of pv modules and corresponding converters
WG	Wind turbine
η_{WG}	Efficiency of wg and corresponding converters
A_{WG}	Total swept area of wg
C_n	Total capacity of batteries
C_{bat}	Capital cost of batteries
C_{bat}	Nominal capacity of batteries
C_h	Capital cost per height of wg tower
C_{PV}	Capital cost of photovoltaic module
C_{WG}	Capital cost of wg
$C_{biogenerator}$	Capital cost of bio generator
$C_{digester}$	Capital cost of digester
D	Diffuse component of hourly global radiation
FF(t)	Fill factor

$G(\beta,t)$	Global solar irradiance on a pv module at a tilt angle of β
V_{Bio}	Volume of biogas supplied to the biogas engine
Cal_{Bio}	Calorific value of biogas
η_{Bio}	Efficiency of bio engine
P_{Biogas}	Power produced by biogas
STC	Standard Test Conditions
SC	Short Circuit
PV	Photo voltaic
h	Wind turbine installation height
I_{SC-STC}	Short circuit current under stc
$I_{SC}(t,\beta)$	Short circuit current of a PV module
K_T	Sky clearness index
K_I	Short circuit temperature coefficient
K_V	Open circuit voltage temperature coefficient
M_{bat}	Annual maintenance cost of battery
M_h	Annual maintenance cost per height of a wg tower
M_{PV}	Annual maintenance cost of a pv module
$M_{Biogenerator}$	Annual maintenance cost of bio engine
$M_{digester}$	Annual maintenance cost of digester
M_{WG}	Annual maintenance cost of a wg
N_P	Number of photovoltaic modules connected in parallel
N_S	Number Of Photovoltaic Modules Connected in Series
N_{Bat}	Total Number of Batteries in A System
N_{bio}	Total Number of Bio Engines
E_{max}	Maximum Charge of The Battery
E_{Cap_max}	Maximum charging capacity
E_{Cap_min}	Minimum discharging capacity
SOC_{max}	Maximum soc limit

SOC_{min}	Minimum soc limit
N_{Pbat}	Total number of batteries in parallel
N_{PV}	Number of photovoltaic modules
N_{Sbat}	Number of batteries connected in series
NCOT	Nominal cell operating temperature
$P_{available}$	Power Available from The System
P_r	Rated power
P_{LOAD}	Load demand
P_{PV}	Power Produced by PV Modules
P_{WG}	Power Produced by Wgs
P_W	Specific Power Output of A WG
T_A	Ambient temperature
v	Wind Speed at Hub Height
V_{bat}	Nominal Voltage of Each Individual Battery
V_{BUS}	Dc bus voltage
v_{ci}	Cut in speed of wg
v_{co}	Cut out speed of wg
$V_{OC\text{-}STC}$	Open circuit voltage under stc
$V_{OC}(t,\beta)$	Open Circuit Voltage at A Particular Hour And Tilt Angle
v_{ref}	Wind Speed at Reference Height
v_r	Rated speed of wind turbine
y_{bat}	Expected Number of Battery Replacements During the Life Of HRES
DOD	Depth Of Discharge
BG	Biogas
BM	Biomass
BS	Battery System
DG	Diesel Generator

FC	Fuel Cell
HG	Hydro Generator
PV	Photovoltaic
WG	Wind Turbine Generator
WT	Wind Turbine
ACS	Annual Cost System
HES	Hybrid Energy System
LCE	Levelized Cost of Energy
MOO	Multi Objective Optimization
PSO	Particle Swarm Optimization
SI	Social Intelligence
RES	Renewable Energy System
SOC	State Of Charge
SOO	Single Objective Optimization
STC	Standard Test Condition
TMY	Typical Methodological Year
GAMS	The General Algebraic Modelling System
HOMER	Hybrid Optimization Model For Electric Renewables
HRES	Hybrid Renewable Energy System
LOLE	Loss Of Load Expected
LPSP	Loss Of Power Supply Probability
NREL	National Renewable Energy Laboratory
DOIRES	Determining Optimum Integration Of RES
GRHYSO	Grid-Connected Renewable Hybrid Systems Optimization
ORIENTE	Optimization Of Renewable Intermittent Energies With Hydrogen For Autonomous Electrification
MENR	Ministry Of Energy And National Resources
SMES	Semiconducting Magnetic Energy Storage

GA	Genetic Algorithm
ANN	Artificial Neural Networks
TS	Tabu Search
SA	Simulated Annealing
NISSO	Novel Improved Social Spider Optimization
OPF	Optimum Power Flow
SSO	Social Spider Optimization
AO	Aquila Optimizer
POA	Pelican Optimizer Algorithm
DOA	Dandelion Optimization Algorithm
GOA	Gazelle Optimization Algorithm
PSR	Predator Success Rate
CF	Cumulative Effect Of Predator
ZOA	Zebra Optimization Algorithm
OOA	Osprey Optimization Algorithm

Chapter 1
Introduction

1.1 The Importance of Diversifying Energy Sources

In a world driven by the relentless pursuit of progress, our dependence on non-renewable energy sources has reached alarming levels. Raw fossil fuels and natural gas, the stalwarts of our energy generation, have propelled us forward for decades, powering our cities, fueling our vehicles, and driving innovation. Yet, this reliance on finite resources has come at a staggering cost.

As our population continues to surge and technologies advance at breakneck speed, our energy consumption has skyrocketed. In just over half a century, it has surged by a staggering 51.8% [1, 2]. This insatiable appetite for energy has left a gaping ecological deficit in its wake, one that has been growing since the 1970s[3, 4]. The consequences have been dire, with environmental disasters and tragedies becoming all too common.

But it doesn't end there. Our addiction to non-renewable energy has also hastened the ominous specter of global warming. The Earth's temperature, once rising at a modest rate, has now spiraled out of control. In the span of a century, it has more than doubled its ascent, leaving 2021 as the sixth hottest year ever recorded[5, 6]. The signs are clear: we are teetering on the edge of an environmental precipice.

To restore balance and safeguard our planet, we must turn to alternatives that offer hope and redemption[7]. Enter renewable energy sources[8]: the champions of a cleaner, greener future. Solar energy, hydro energy, wind energy, biomass, and biogas have emerged as beacons of possibility, offering efficient and sustainable means of power generation[9]. These sources, when harnessed together in hybrid systems, possess the power to transform our energy landscape, providing us with abundant electricity while treading lightly on the Earth.

But the benefits extend beyond environmental stewardship. Though the initial costs of implementing renewable energy power plants may seem daunting, the long-term advantages are undeniably compelling[10]. By eliminating the burden of fuel costs and associated charges, these systems prove their cost-efficiency over time. The investment is recouped within a few short years, paving the way for profitability and a secure energy future[11, 12].

In a world yearning for a harmonious equilibrium, renewable energy sources hold the key to unlocking a brighter tomorrow. They present us with an unparalleled opportunity to meet our ever-growing energy needs sustainably and responsibly. It's time to harness their immense potential and embark on a transformative journey towards a cleaner, greener, and more prosperous future for all.

1.2 Literature Review

As we speculated the amount of carbon emission[13] in the year of 2022 to be around 107 million tons[14], so the renewable energy sources are the best solution to global warming and reduction of fossil fuel[15]. Sustainable Energy Development Strategies typically involve three major technological changes[16], energy savings on the demand side , efficiency improvements in the energy production and replacement of fossil fuels by various sources of renewable energy. Consequently, large-scale renewable energy implementation plans must include strategies for integrating renewable sources in coherent energy systems influenced by energy savings and efficiency measures the available renewable energy sources that are used [8, 17]:

1. Solar Energy

2. Wind Energy
3. Biomass
4. Hydropower
5. Geothermal

Each of these renewable sources has different power generation rate based on geographical locations and environment but the table 1.1 shows the contribution of RE sources way back in 2001[18].

Table 1.1: Energy generation from RE sources.

Resource	Annual Delivered Energy (kwh/m^2)
Wind Energy (intermittent)	11(avg. wind speed); 18(high wind speed)
Biomass (baseload)	15(low efficiency); 45(high efficiency)
Photovoltaics(intermittent)	50-100
Geothermal (The Geyser) (baseload)	160-200

We can see the contribution of renewable energy goes way back and has developed quickly. The Ministry of Energy and National Resources (MENR) encourages to increase the share of RES in electricity generation, and it is striving to improve the whole capacity of renewables to 61,000 MW by 2023[19]. 34,000 MW of this total installed generation will be composed of hydropower; 20,000 MW of wind power, 1000 MW of geothermal, 5000 MW of solar, and 1000 MW of biomass energy. The total estimated cost of this object is almost 60 billion dollars (about $180 per person in the US). Table 1.2.2 shows the estimated resource-based electricity generation rates in the 2023 MENR strategic plan[19].

Table 1.2 : 2023 MENR Strategic Plan: Projected Electricity Generation

Renewable Energy Sources	2015	2017	2019	2023
Hydropower	25,526	28,763	32,000	34,000
Wind	5660	9549	13,308	20,000
Geothermal	412	559	706	1000
Solar	300	1800	3000	5000
Biomass	377	530	683	1000
Total	**32,275**	**41,241**	**49,697**	**61,000**

1.2.1 Hybrid Renewable Energy System(HRES)

As we can see, this field's most recent advancements and research have enhanced both manufacturing volume and cost effectiveness. The capacity and efficiency of electricity generation have even increased thanks to the development of hybrid renewable energy systems(HRES) .The HRES is a novel type of power generation that combines two or more renewable energy sources with conventional ones. Any combination of renewable resources may be used. Nature's renewable energy sources are constantly in a precarious intermittent situation. The development of HRES included a hybrid combination of storage (also known as a battery), Semiconducting Magnetic Energy Storage (SMES), and water storage as a possible hydro turbine[20].

1.2.2 Research on HRES

According to a study from 2023[21],Indonesia possesses a tropical environment with abundant solar radiation, making it an ideal candidate for solar power production. However, the country has not fully utilized its renewable energy resources. The study highlights that the current usage of solar, wind, and biomass energies in Indonesia is only 5.1%, 0.04%, and 0.01%, respectively, despite their significant capacities of 32,654 MW, 207,898 MW, and 60,647 MW. Recognizing the potential for economic gain and emissions reduction, Indonesia's national energy strategy aims to capitalize on these natural resources and address its electricity access challenges.

In a case study region with a daily load demand of 890 kWh and a peak load of 167.2 kW, an off-grid hybrid system consisting of photovoltaic (PV) panels, a bio generator, a diesel generator, batteries, and the grid was recommended[21]. This combination optimally addressed the region's energy needs. The study's optimization findings indicate a Net Present Cost (NPC) of $1.02 million and a Levelized Cost of Energy (COE) of 0.188 $/kWh for the average cost of usable energy produced by the system. The NPC measures the present value of a system's lifetime costs of investment and operation[21].

Another research from 2019[22] demonstrated the technological advantages of a hybrid PV-BESS (Battery Energy Storage System) for renewable energy utilization. Furthermore, the paper investigated the feasibility of a Building Integrated PV (BIPV) system with and without a battery.

For rural electrification in the outlying district of Korkadu, India, a study focused on designing an ideal HRES[23]. Solar photovoltaic, wind turbines, and bio generators were considered the primary energy sources due to their abundant potential in the Korkadu district. The study calculated the load forecasts for the chosen district, encompassing residential, commercial, institutional, and agricultural sectors, to ensure reliable electrification.

In order to harness useful outputs such as power, hydrogen, hot water, and clean water, a study proposed a novel flash-binary geothermal power plant coupled with a steam cycle and a carbon dioxide-based Rankine cycle (RC), along with a desalination unit and a Proton Exchange Membrane (PEM) electrolyzer[24].

In a distant village named Tazouta in the Moroccan Fez-Meknes region, various freestanding HRES combinations are evaluated for a constant power supply to 10 households[25]. The included solar, wind, and biomass energy sources. The best configuration scenario, denoted as A (PV-Wind-Biomass-Battery), yielded a unit energy cost of 0.2 $/kWh for an average energy requirement of 91.38 kWh/day and a peak load of 6.44 kW. Therefore, the proposed system offers a promising solution for ensuring energy supply security.

According to papers[26-28] , the most cost-efficient HRES combination is PV-WT-BS (photovoltaic, wind turbine, and battery storage). These studies utilize six optimal sizing methods to determine the appropriate configuration.

On the other hand, papers[29-32] explored the HRES combination of PV-WT-DG-BS (photovoltaic, wind turbine, diesel generator, and battery storage). Different algorithms were employed to optimize the sizing of this system configuration.

1.2.3 Sizing Methodologies for HRES

The sizing of HRES is very important as it combines different RE sources[33, 34]. The sizing has to be perfect so that it is cost efficient as well as it satisfies the load demand .The main methodologies are as follows[35]:

1. Graphic construction method
2. Probabilistic method
3. Artificial intelligence method
4. Iterative method
5. Hybrid method

1.2.3.1 Graphic construction method

A graph-making approach involves balancing the average value of the HRES system's generation with the average value of the load demand. It is necessary to employ graphical representations of a sizing curve between the potential sizes of HRES and load demand. Borowy and Salameh developed a graphical method for calculating the required size of PV modules and batteries depending on wind speed and solar radiation for each hour of the day. This hybrid system design was used to meet the load demand in a Massachusetts home. The quantity of PV modules and LPSP batteries was determined by the cost of the system[36].

1.2.3.2 Probabilistic method

The selection of the optimal size of the microgrid components is one of the most essential power system aspects, and probabilistic techniques are one of the finest options for sizing[37].

It should be noted that insufficient component sizing can lead to problems such as microgrids functioning badly in terms of total loss, total cost, load supply, and long-term battery bank cell deterioration. Because of the intermittent nature and unpredictable output of renewable energy sources, ESSs should be used to avoid any negative impacts and increase electrical energy use[38].

1.2.3.3 Iterative method

This approach's performance for HRES is computed using a recursive procedure that ends when the ideal configuration is achieved based on the design criteria. The recursive procedure used to evaluate iterative approaches for HRES reaches a conclusion when the best configuration meets the design requirements[39]. Yang et al. proposed for a hybrid wind-solar power system based on COE and levelized cost of energy (LCE)[39].

1.2.3.4 Artificial intelligence method

Machine learning algorithms influenced by human concepts are included in AI[40]. Researchers used a variety of AI technologies to improve HRES and reduce energy consumption, including Fuzzy Logic, genetic algorithms (GA), and artificial neural networks (ANN)[41]. Kumar et al. created a hybrid system that used solar, wind, and diesel to lower the overall cost of the HRES[42].

1.2.3.5 Hybrid methods

Hybrid solutions effectively integrate two or more diverse strategies to provide the best feasible solution for the specific situation. The employment of a hybrid technique is more common in multi-objective settings when two or more variables are optimized at the same time[43]. Arabali et al. [44]presented a hybrid technique based on HRES for assessing the stochastic performance and sizing of PV-wind-batteries. The auto regressive moving average (ARMA) technique was used to stochastically evaluate the intermittent nature of PV and wind power producing systems[45, 46]. To examine the system's dependability and cost-cutting potential, the pattern search (PS) and sequential Monte Carlo simulation (SMCS) methodologies were combined. Instead of implementing Tabu Search (TS) and Simulated Annealing (SA) separately, the proposed optimization strategies used a hybrid mix of the TS and SA algorithms to get enhanced convergence and optimal outcomes[47]. The hybrid model is the best option for microgrid design in rural and isolated places, according to the researchers' theoretical analyses of different sizing methodologies[48, 49].

There are other ways to categorize methodologies[50, 51].

1. Software tools
2. Evolutionary algorithms
3. Nature inspired algorithms

4. Linear programming
5. Dynamic programming I
6. Matrix approach
7. Design space-based approach

1.2.4 Softwares Related To HRES Sizing

Due to multiple generation systems, hybrid system analysis is quite complex and requires to be analyzed thoroughly. This requires software tools for the design, analysis, optimization, and economic viability of the systems. The software studied are[52]

1. HOMER[53-56]	2. Hybrid2	3. RETScreen
2. iHOGA	5. INSEL	6. TRNSYS
7. iGRHYSO[57]	8. HYBRIDS	9. RAPSIM
10. SOMES	11. SOLSTOR	12. HySim
13.HybSim	14. IPSYS	15. HySys
16.Dymola/Modelica	17. ARES	18. SOLSIM
19.HYBRID DESIGNER.		

Fig 1.1 : Schematic representation of HOMER

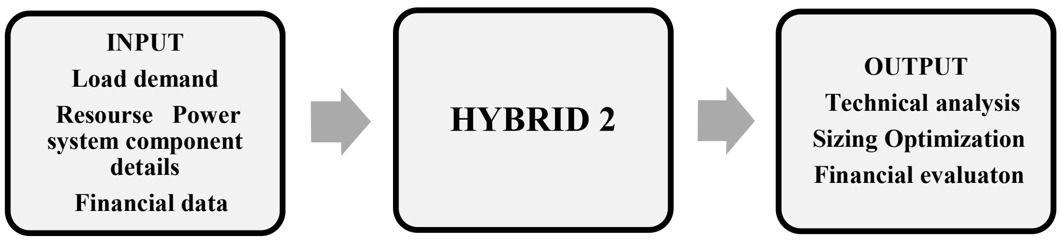

Fig 1.2 : Schematic representation of HYBRID 2

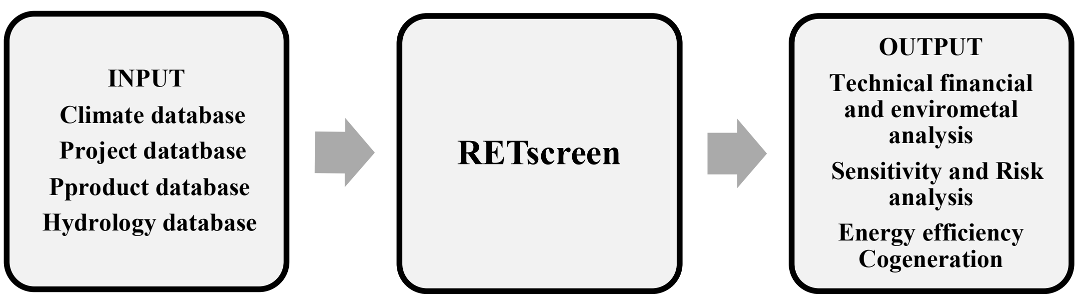

Fig 1.3 : Schematic representation of RETScreen

Fig 1.4 : Schematic representation of iHOGA

1.2.5 Single Objective Optimization (SOO)

Single objective optimization focuses on satisfying only one objective, there is only one objective function. The objective function may contain multiple optimization parameter and each of them is linked through it. Each optimization parameter will have constraints of its own[58, 59].

There are many researches in this field. Here are some examples:

The author of this paper used, differential evolution (DE) ,a new evolutionary optimization algorithm that has been shown to be fast and simple for unconstrained single-objective optimization problems[60, 61].

The research offers a novel improved social spider optimization method (NISSO) for solving the optimum power flow (OPF) issue by optimizing electricity generating fuel cost, power loss, polluted emission, voltage deviation, and L index separately[62, 63]. In the study, the suggested NISSO approach is initially created by executing three changes with the goal of improving optimal solution quality and speeding up convergence of traditional social spider optimization (SSO).Here the conception of single objective optimization is used for the algorithm[64, 65].

In[66] an SOO based methodology was presented for sizing stand-alone PV/WG system. The overall system cost over a 20-year period was equal to the sum of the corresponding component capital and maintenance expenses[67, 68].

Similar research work has been done in this paper as well using genetic algorithm and SOO[69].

A method for optimal sizing and strategy control was described in this where differential flatness approach was applied. The method included the concept of SOO in optimization[70, 71]

There are more researches based on single objective optimization. In our thesis, we have used single objective optimization where one objective function addresses the optimization parameters.

1.3 Thesis objectives:

i. To propose an optimization technique for a wind-photovoltaic-biogas-battery hybrid renewable energy system that is the most cost-effective and guarantees zero power supply probability.

ii. To compare several optimization algorithms recently presented for a wind-photovoltaic-biogas-battery hybrid renewable energy system.

Chapter 2

Mathematical Model and Problem Formulation

The studied HRES consists of WT, PV, Biomass and batteries are used as storage component. The chapter begins by demonstrating how these components are linked to one another. These components are introduced further, along with their mathematical equations. These components' specifications for this study are also provided. The objective function based on LPSP is presented at the end of this chapter.

2.1 System Architecture

When different energy sources are used to produce electricity, the system is known as a hybrid renewable energy system (HRES). A HRES can be built using both renewable and non-renewable energy sources. However, since this idea was developed with the intention of replacing nonrenewable sources of energy, HRES primarily focuses on the usage of renewable sources of energy. The utilization of numerous sources is required to stabilize the system because, in contrast to non-renewable energy sources, renewable energy is unpredictable. Undoubtedly a system consisting of multiple energy sources provides much more reliability in terms of cost and efficiency in comparison to a system consisting of a single source of energy[72, 73]. Furthermore, due to the rise in the price of petroleum goods, HRES that use renewable energy are gaining appeal, particularly in distant places[74]. Researchers throughout the world use a variety of energy sources, including hydrogen, fossil fuels, HG, geothermal, BM, BG, WT, and solar energy used in PV cells along with energy storage systems[75, 76]. The literature review suggests that PV-WT-BG-BS is the most cost effective and cleanest combination among all of them[77].

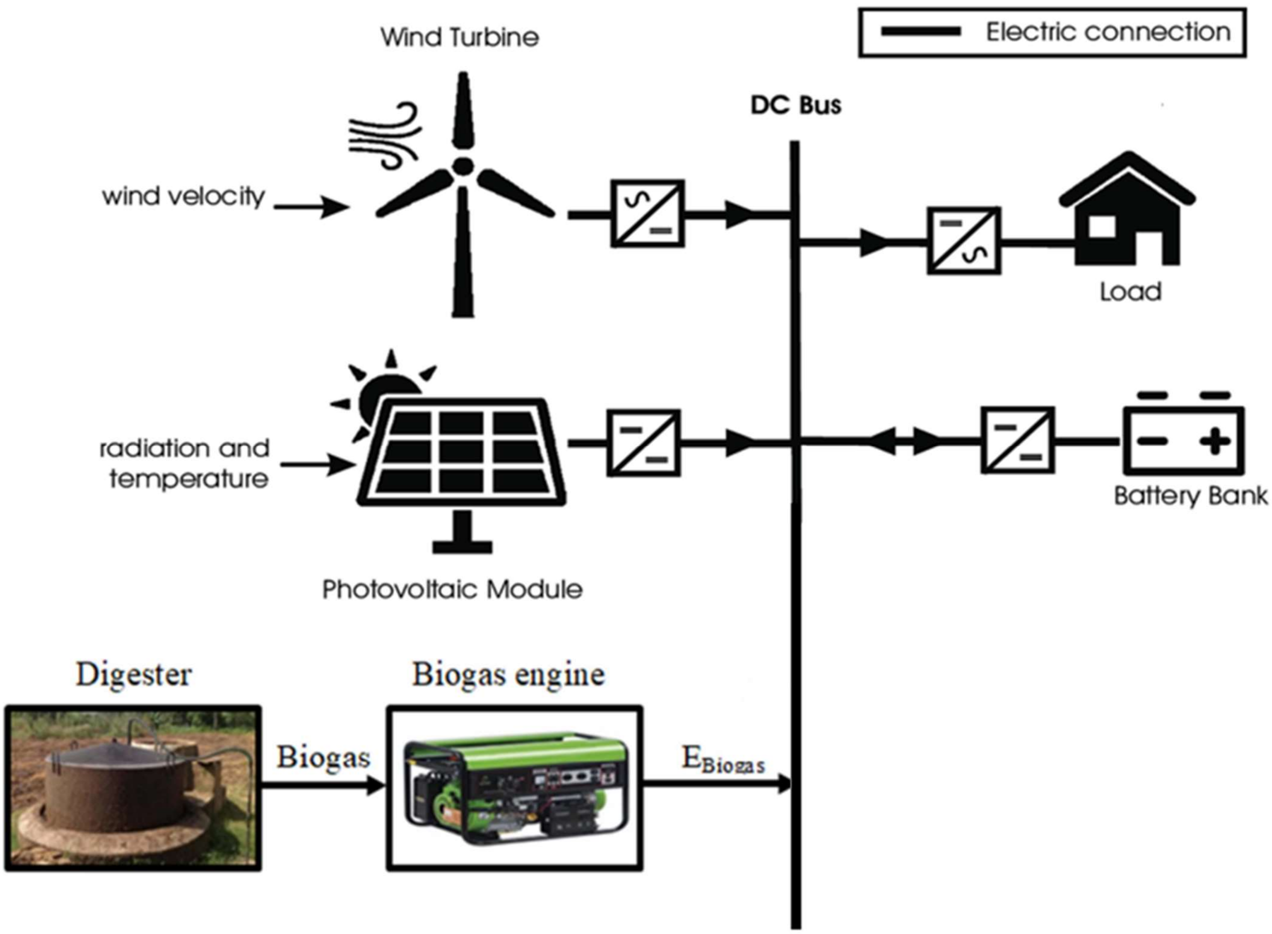

Fig. 2.1: A PV-WT-BG-BS hybrid renewable energy system

In this study, the HRES consists of three sources of energy which are wind generator, photovoltaic cells and biogas generator and as an energy storage system, a battery storage system is employed. Each of the components is discussed below:

2.2 Mathematical Model

2.2.1 Wind Turbine Model

For the HRES, any wind turbine may be chosen. The non-linear power characteristics curve provided by the manufacturer of the particular wind turbine, however, should be used to analyze the type of wind turbine that was selected. A typical power curve is presented in Fig 2.2 to provide an insight into the behavior of a wind turbine.

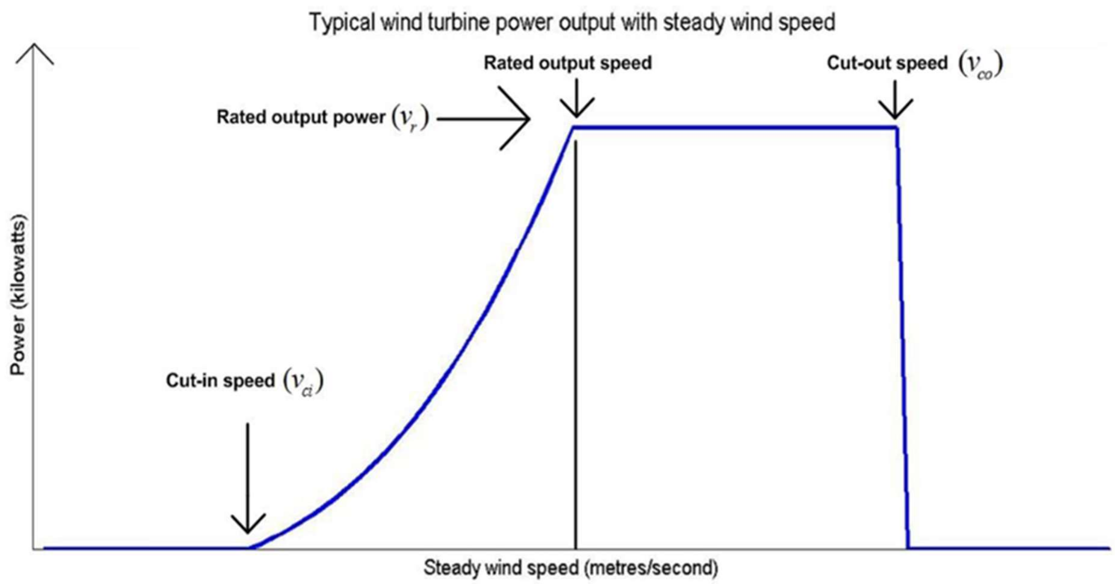

Fig. 2.2: Wind turbine power output characteristics

From Fig. 2.2 it is obvious that wind speed of a particular site plays a vital role for generating power. The Typical Meteorological Year (TMY) data can be used to calculate the wind speed at a reference height (about 33m) of the research location. Based on the study by[78-81], the specific power output, P_w (W/m^2), depends on the wind speed at that location and is expressed as,

$P_w(t) = 0 \qquad\qquad v(t) < v_{ci}$

(2.1)

$P_w(t) = av^3(t) - bP$ $\quad\quad v_{ci} \leq v(t) < v_r$

$P_w(t) = P_r$ $\quad\quad v_r \leq v(t) < v_{co}$

$P_w(t) = 0$ $\quad\quad v(t) \geq v_{co}$

Where,

$$a = \frac{P_r}{v_r^3 - v_{ci}^3},\ b = \frac{v_{ci}^3}{v_r^3 - v_{ci}^3}$$

v_{ci} = cut in speed of the WG

v_r = rated speed of the WG

v_{co} = cut out speed of the WG

P_r = rated power of WG

Cut in, rated, cut out speed of the wind turbine and the rated power of the WG can be found from the manufacturer of the selected turbine.

The wind velocity at hub height is required to implement the above equation. The following equation is used to calculate velocity at a given height[79, 80].

$$V_h = V_r \left(\frac{\mathrm{h}}{\mathrm{hr}}\right)^{\alpha} \quad (2.2)$$

In equation 2.2,

v_r = windspeed at the reference height; v_h = windspeed at the hub height.

α = power law coefficient

h = WG installation height; h_r = reference height

From[81], it can be concluded that

$\alpha < 0.10$ for flat land, water and ice

$\alpha > 0.25$ for heavily forested landscape

For this study $\alpha = 0.15$ is taken, as [79] implies, the site being studied is a decent approximation for such an area because it almost resembles an open topography of grasses. So, after taking into account all of the aforementioned information, it can be said that the actual electric power production as obtained from a wind turbine is represented by

$$P_{WG} = P_w A_{WG} \eta_{WG} \qquad (2.3)$$

In equation 2.3,

P_{WG} = Power produced by WG

A_{WG} = total swept area by WG

η_{WG} = efficiency of WG

The details of the considered WT are given in the Table 2.1[80]

Table 2.1 : Specifications of Wind Turbine

Power (W)	**h_{low}(m)**	**h_{high} (m)**	**WG capital cost ($)**	**Tower capital cost ($/unit length)**
1000	11	40	2400	55

2.2.2 Photovoltaic (PV) module model

This is the second renewable energy source used in this research. It should be emphasized that PV modules cannot generate any power at night because they are dependent on solar radiation to do so. The power generation of PV modules is influenced by factors besides solar radiation, such as ambient temperature and irradiation conditions, and these characteristics vary from module to module. The manufacturer of the photovoltaic modules supplies this data for the standard test conditions (STC) 25 C cell temperature and 1 kW/m2 solar irradiance). By incorporating these manufacturer data, the output power of a PV module at any one time is determined by the following equation [69]

$$P_{PV}(t,\beta) = N_s.N_p.V_{oc}(t,\beta).I_{sc}(t,\beta).FF(t)$$

$$V_{oc}(t,\beta) = \{ V_{OC\text{-}STC} - K_v T_c(t) \}$$

$$I_{sc}(t,\beta) = \{ I_{SC\text{-}STC} + K_I[T_c(t) - 25°C] \} \frac{G(t,\beta)}{1000} \quad (2.4)$$

$$T_c(t) = T_A + (NCOT - 20°C) \frac{G(t,\beta)}{1000}$$

In equation 2.4,

P_{PV} = Power produced by the PV modules

β = Tilt angle of PV

N_s = number of PV modules connected in series

N_p = number of PV modules connected in parallel

V_{oc} = Open circuit voltage

I_{sc} = Short circuit current

FF = Fill factor (ratio of actual P_{max} to the product of V_{oc} and I_{sc})

K_v = Open circuit voltage temperature coefficient

K_I = Short circuit current temperature coefficient

G = Global solar irradiance

T_A = Ambient Temperature

NCOT = Nominal cell operating temperature

It is clear from equation 2.4 that we require the value of incident global solar irradiance on the PV module. Although hourly global irradiance on a horizontal plane can be found in meteorological year (TMY) data sets, it is insufficient for this investigation because the PV modules are not arranged horizontally. The solar irradiance is divided into beam and diffuse components for a slanted PV module.

Hourly clearance index, $k_T = \frac{G(beam)}{D(diffuse)}$

Where, ratio of beam(G) and diffuse(D) can be expressed in terms of

$$\frac{G}{D} = \begin{cases} 1.0 - 0.09\, k_T & 0 < k_T < 0.22 \\ 0.9511 - 0.1604 k_T + 4.388\, k_T^2 - 16.638 k_T^3 + 12.336 k_T^4 & 0.22 < k_T \leq 0.80 \\ 0.065 & k_T > 0.8 \end{cases} \quad (2.5)$$

$$R_b = \frac{\cos(\varphi+\beta)\cos\delta\cos\omega+\sin(\varphi+\beta)\sin\delta}{\cos\varphi\cos\delta\cos\omega+\sin\varphi\sin\delta} \quad (2.6)$$

In equation 2.6, R_b is a geometric factor that represents the ratio of beam radiation on a slanted surface to that on a horizontal surface at any given time.

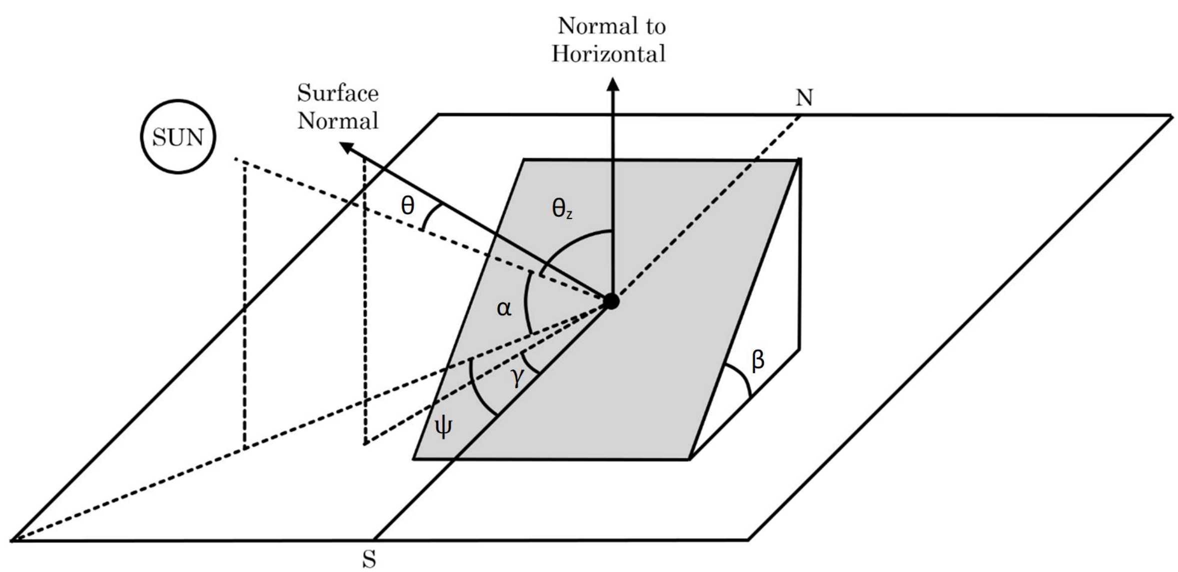

Fig.2.3 : *Angles related to the sun*

To understand the angles associated in equation 2.6 let us take a look at Fig. 2.3. φ is the latitude of this site, β is the tilt angle of the PV module. From Fig. 2.3 it is seen that the PV module is titled at β degree from the horizontal surface. The hour angle, denoted as ω, represents the amount of angular displacement of the Sun, measured in degrees, towards the east or west of the local meridian due to the Earth's rotation on its axis at a rate of 15° per hour. Therefore, in the afternoon, the hour angle is positive, and in the morning, it is negative.

The angle of declination, denoted by δ, represents the Sun's position at solar noon relative to the equator. It ranges from -23.45° to 23.45° and is positive in the northern hemisphere and negative in the southern hemisphere. It impacts the amount of solar radiation received by a location, with greater angles resulting in more intense radiation. The declination angle is represented by equation

$$\delta = 23.45 \sin\left(360 \frac{284 + n}{365}\right) \tag{2.7}$$

In equation 2.7, n is the day of the year. Incorporating tilt angle of PV, the total hourly global radiation can be found from the following equation [82]

$$G(t, \beta) = (G - D)R_b + D\left(\frac{1+cos\beta}{2}\right) + G\rho_g\left(\frac{1-cos\beta}{2}\right) \tag{2.8}$$

In the equation 2.8 ρ_g is called the ground reflectance. Total power output from the PV can be determined from the following expression

$$P_{array(t,\beta)} = \eta_{PV} N_S N_P P_{PV}(t, \beta) \tag{2.9}$$

Where, η_{PV} is the efficiency of the converter of pv. It should be noted that in the current study, the magnitude of the DC bus voltage determines the number of PV modules in series, whereas the number of PV modules in parallel is determined by the optimization algorithm.

The details of the considered PV module are given in Table 2.2 [80]

Table 2.2: Specification of PV module

V_{OC} (V)	I_{SC} (A)	V_{max} (V)	I_{max} (A)	P_{max} (W)	Capital Cost ($)
64.8	6.24	54.7	5.86	320	640

2.2.3 Biogas Modelling

It serves as the 3rd renewable energy source in this study. Anaerobic digestion is a valuable waste management process that utilizes microorganisms to break down biodegradable material, producing biogas which can be utilized as a sustainable energy source. The study employed a fixed digestor dome[83] and food waste with a gas production rate of 0.05 m3/kg[84]. This technique is crucial due to the surge in global waste production caused by urbanization and population growth, resulting in the need for sustainable solutions. The output power of a biogas model is determined using the following equations[85]

$$Gas_{produced} = Food\ waste\ (kg) * Gas_{production\ rate}\ (m^3/kg) \tag{2.10}$$

$$P_{Biogas} = \frac{V_{Bio} * Cal_{Bio} * \eta_{Bio}}{860} \tag{2.11}$$

In the equation 2.10, 2.11,

V_{Bio} = Volume of biogas supplied to biogas engine

Cal_{Bio} = Calorific value of biogas

η_{Bio} = Efficiency of Bio engine

P_{Biogas} = Power produced by the Biogas engine

The details of the considered Biogas engine are given in Table 2.3

Table 2.3: Specification of the Biogas Engine

Power (W)	Biogas Engine Capital Cost ($)	Digestor volume (m^3)	Digestor Capital Cost ($)
3000	720	22.183	2550

2.2.4 Battery Model

The selected sources of energy are inherently variable, leading to fluctuations in electricity generation that may exceed or fall short of current demand. Ensuring consistent and stable operation of energy storage systems requires an energy storage system capable of storing excess energy and releasing it as needed. This is achieved through the use of a battery that charges and discharges in response to current conditions.

The state of charge (SOC) of the battery is critical to maintaining optimal energy balance within the system. Accurate determination of the SOC requires understanding of the initial SOC level, charging or discharging duration, and current flow magnitude. An equation can be used to determine the SOC at any given time

$$I_{bat}(t) = \frac{P_{PV}(t) + P_{WG}(t) - P_{Load}(t)}{V_{bat}(t)}$$

$$SOC(t) = SOC(t-1).\left(1 - \frac{\sigma.\Delta t}{24}\right) + \frac{I_{bat}(t).\Delta t.\eta_{bat}}{C_{bat}} \tag{2.12}$$

Where,

σ = self-discharging rate of a battery

I_{bat} = Battery Current

C_{bat} = Nominal Capacity of The Battery

η = Charging Efficiency

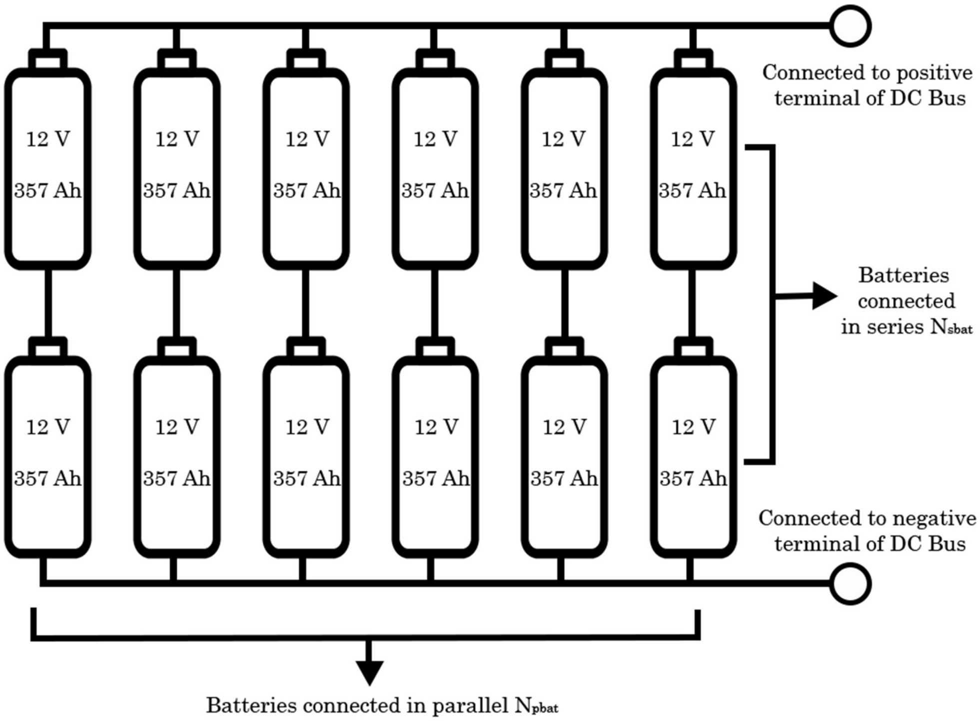

Fig. 2.4: Batteries connected in series and parallel

In reference to[81], sigma is dependent on the cumulative charge and in this study the value is assumed of 0.2%[86]. Furthermore, charging efficiency is fixed at 0.8, while discharging efficiency is set at 1. The total charge of a battery storage system is determined by the nominal charge of the battery and the number of batteries connected in parallel. The number of batteries in series is dependent on the DC bus voltage,

$$N_{bat} = N_{Sbat} \times N_{Pbat}$$

$$N_{Sbat} = \frac{V_{BUS}}{V_{bat}} \tag{2.13}$$

$$C_n = N_{Pbat} \times C_{bat}$$

In equation 2.13,

N_{bat} = Total number of batteries

N_{Sbat} = Batteries connected in series

N_{Pbat} = Batteries connected in parallel

V_{BUS} = DC bus voltage

V_{bat} = Battery voltage

C_n = Total charge of Battery

The authors of [87] assert that the longevity of a battery can be compromised by overcharging and deep discharging. To optimize battery lifespan, it is advised to circumvent these events by refraining from overcharging and critical discharge. In this study, the maximum state of charge (SOC) was set at 1, while the minimum SOC was set at 0.2. The maximum charge and the maximum and minimum charging-discharging capacity can be calculated using following equations[88]

$$E_{max} = (C_n \times V_{bat})/1000$$

$$E_{cap\_max}(t) = (SOC_{max} - SOC(t)) \times E_{max} \tag{2.14}$$

$$E_{cap\_min}(t) = (SOC(t) - SOC_{min}) \times E_{max}$$

The details of the considered battery model are given in Table 2.4

Table 2.4 : Specifications of Battery

Price($)	Voltage(V)	Capacity(Ah)
1239	12	357

2.3 Objective function Formulation

The objective function is formulated on the basis of loss of power supply probability. The economic viability of a Hybrid model is determined by its ability to meet the load demand. This is reflected in the loss of power supply probability (LPSP)[89] which represents the probability that the model will fail to meet the load demand. LPSP ranges from 0 to 1, where 0 indicates complete reliability and 1 indicates complete failure. LPSP is mathematically expressed as a function that governs the probability of power supply failure. LPSP is determined by the following equation[81, 90]

$$LPSP = \frac{\sum_{t=1}^{8760} Loss\ of\ power\ supply\ (t)}{\sum_{t=1}^{8760} P_{Load}\ (t)} = \frac{\sum_{t=0}^{T} Loss\ of\ power\ supply\ time}{T}$$

$$Loss\ of\ power\ supply\ (t) = P_{Load}(t) - P_{generated}(t) \tag{2.15}$$

$$Loss\ of\ power\ supply\ Time = Time\left(P_{generated}(t) < P_{Load}(t)\right)$$

In equation 2.15, T is the total number of hours in a year and $\sum_{t=0}^{T} Loss\ of\ power\ supply\ time$ represents the summation of all the hours during which the available power was less than the demand.

The main objective of this research is to reduce the costs associated with HRES. The LPSP is kept at close to zero, ensuring maximum reliability. After that, the cost is computed, resulting in a single-objective optimization.

This study assumes a 25-year lifespan for the HRES under examination. The associated costs include not only the initial setup cost of the PV, WG, and batteries but also the maintenance cost throughout its operational lifespan. As indicated in reference[91], the objective function can be expressed as follows.

$$
\begin{aligned}
&Minimize\ f(N_{PV}, N_{WG}, N_{bat}, \beta, h, N_{bio}) \\
&\qquad = \big[N_{PV}(C_{PV} + 25M_{PV}) + N_{WG}(C_{WG} + 25M_{WG} + hC_h + 25hM_h) \\
&\qquad + N_{bat}(C_{bat} + V_{bat}C_{bat}) + (25 - Y_{bat} - 1)M_{bat} \\
&\qquad + N_{bio}\big(C_{biogenerator} + 25M_{biogenerator}\big) + C_{digester} \\
&\qquad + 25M_{digester})\big]
\end{aligned} \tag{2.16}
$$

Subject to the constraints

$N_{WG} > 0$

$N_{PV} > 0$

$N_{bat} > 0$

$N_{bio} > 0$

$90° \geq \beta \geq 0$

$11 \geq h \geq 40$

In equation 2.16 $N_{PV}, N_{WG}, N_{bat}\ and\ N_{bio}$ are the number of PV modules, WGs, batteries and bio-engines respectively, C_{PV}, C_{WG}, C_{bat}, $C_{biogenerator}$ $and\ C_{digester}$ are the capital cost of PV modules, WGs, batteries and bio-engines respectively,$M_{PV}, M_{WG}, M_{bat}, M_{biogenerator} and\ M_{digester}$ are the annual maintenance cost of PV modules, WGs, batteries, bio-engines and digester respectively, C_h is the capital cost per unit height of WG tower, M_h is the yearly maintenance cost per unit height of a WG tower and Y_{bat} is the expected number of battery replacements during the life of HRES.

2.4 Methodology

To begin the optimization process, several initial parameters are loaded, such as solar irradiance, wind velocity, load demand, and food waste. The population and algorithm parameters are then initialized. The simulation starts by generating six random solution sets: $N_{PV}, N_{WG}, N_{bat}, \beta, h\ and\ N_{bio}$. These sets have defined upper and lower bounds. The generated data is fed into corresponding models to calculate the power generated by each model, thereby determining the total generation.

Next, the algorithm checks if the total generation meets the total demand. If the power generated exceeds the load demand, the surplus energy is stored in the battery energy storage for later use. On the other hand, if the generation falls short of the load demand, the deficit amount of energy, or a partial amount, can be supplied by the battery energy storage. If there is still a shortfall in energy demand, it is considered unmet energy.

This energy monitoring process continues for a year, after which the system calculates the Loss of Power Supply Probability (LPSP) and checks if it equals zero. If LPSP is zero, the system calculates the value of the fitness function. If the maximum number of iterations has not been reached, the entire process repeats. All these procedures are illustrated below using flow diagrams in fig 2.4(a), 2.4(b), 2.4(c).

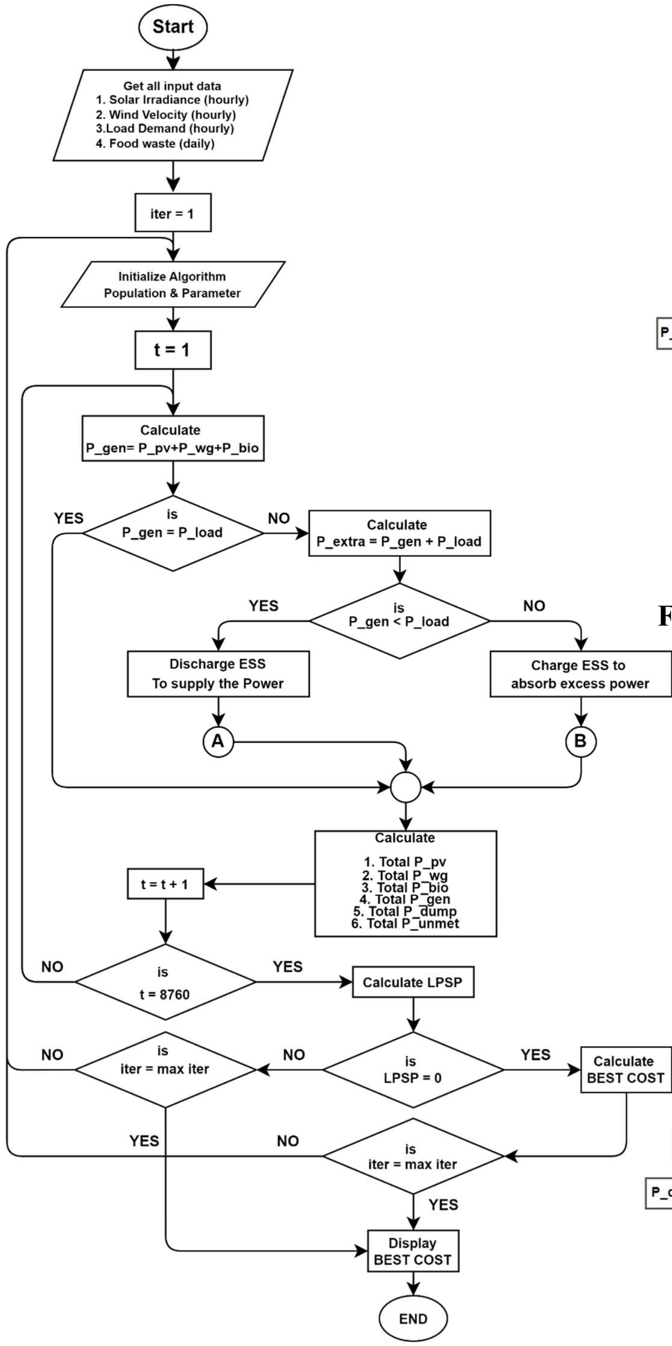

Fig 2.5 (a) : Overall Methodology of the Entire Study

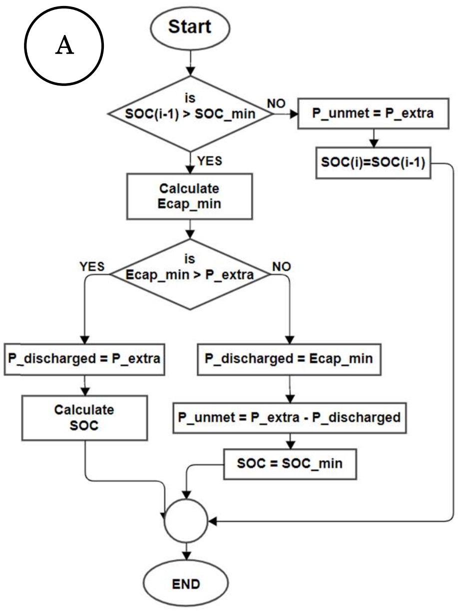

Fig 2.5 (b) : ESS Discharging(A)

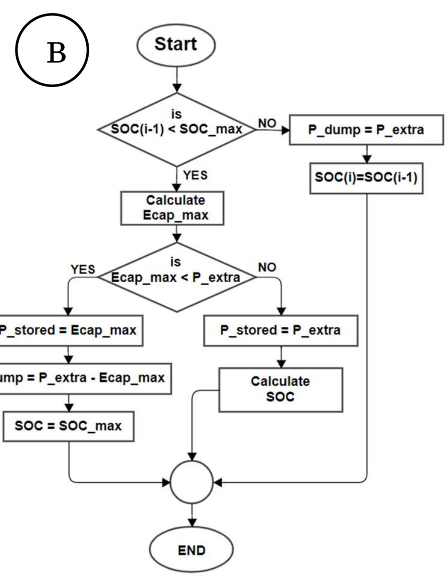

Fig 2.5(c) : ESS Charging(B)

In summary, the optimization process involves iteratively generating random solution sets, calculating power generation, checking energy balance, storing or discarding surplus energy, supplying energy from the battery, monitoring energy demand for a year, calculating LPSP, evaluating fitness function, and repeating until the maximum number of iterations is reached.

2.5 Summary

The Hybrid Renewable Energy System (HRES) and the objective functions linked with it have been explained. The HRES is clearly extremely dependent on the environmental conditions of the implementation site. As a result, including an energy storage device becomes vital, but it also raises the system's cost. As a result, optimizing the consumption of generated energy in an economically viable manner is critical.

Chapter 3

Study of Optimization Algorithm

3.1 Particle Swarm Optimization

Particle Swarm Optimization (PSO) is a nature-inspired optimization technique that uses a swarm of interacting particles to explore a search space and find the optimal solution[92, 93]. These particles, inspired by social swarms like bees and ants, exhibit decentralized control and cooperation to achieve emergent behavior at a global level[92, 93] . Social Intelligence (SI), a subset of AI, models the collective behavior of social swarms such as bird flocks and ant colonies[94]. Through verbal or visual communication, like the honey bees' waggle dance, or indirect interaction through environmental changes, such as ants leaving pheromone trails, swarms efficiently perform essential tasks[95]. PSO, one of the popular SI models, mimics the flocking behavior of birds. It iteratively updates particle positions based on personal best (P_{best}) and global best (G_{best}) positions to converge towards the optimal solution[96]. Assuming a minimization problem,

$$P_{best_i}^{t} = x_i^* \mid f(x_i^*) = \min\left(\left\{f\left(x_i^k\right)\right\}\right) \quad k = 1, 2, 3 \dots \dots, t$$
$$where\ i \in \{1, 2, \dots, N\}, and \tag{3.1}$$

$$g_{best}^{t} = x_*^t \mid f(x_*^t) = \min\left(\left\{f\left(x_i^k\right)\right\}\right)$$
$$where\ i = 1, 2, 3, \dots, N\ and\ k = 1, 2, \dots, t \tag{3.2}$$

Here,

i = particle's index,

t = current iteration

f = objective function to be optimized

x = position vector

N = total number of particles in the swarm

The following equations update the velocity v and position x of each particle i at each current iteration t+1 as follows :

$$v_i^{t+1} = wv_i^t + c_1r_1\left(P_{best_i}^t - x_i^t\right) + c_2r_2(g_{best}^t - x_i^t) \qquad (3.3)$$

$$x_i^{t+1} = x_i^t + v_i^{t+1} \qquad (3.4)$$

Where, v represents the velocity vector, w is the inertia weight used to balance local and global exploration, r1 and r2 are random vectors uniformly distributed within the range [0,1] and c1 and c2 called "acceleration coefficients" are positive constant. The "velocity clamping" method[97] prevents particles from reducing their search space and encourages exploration across the full domain during optimization by setting an upper constraint for the velocity vector.

Table 3.1 contains step by step instructions for coding PSO

Table 3.1 : Pseudocode of Particle Swarm Optimization

```
Initialize particles' positions and velocities
Initialize global best position and fitness

While termination condition is not met:
  For each particle :
     Update particle's velocity using the formula:
        velocity = (inertia weight) * velocity
           + (cognitive weight) * rand() * (particle's best position - current
           position)
           + (social weight) * rand() * (global best position - current position)

     Update particle's position using the formula:
        position = position + velocity

     Calculate fitness of the new position

```

```
        If the new position is better than the particle's best position:
            Update particle's best position

        If the new position is better than the global best position:
            Update global best position

    Update termination condition (max. number of iterations or target fitness value)

Return global best position and fitness
```

3.2 Aquila Optimizer

The Aquila, an extensively studied bird, excels in hunting with its speed and sharp talons. When hunting solo, male Aquila capture a significant amount of prey. They employ four different hunting methods and can quickly adapt between them depending on the situation. Their prey includes squirrels, rabbits, and even full-grown deer[98]. It involves three stages in its operation.

Expanded Exploration

$$X_1(t+1) = X_{best}(t) \times X_{best}\,(1 - \frac{t}{T}) + (X_M\,(t) - X_{best}\,(t) \times rand) \qquad (3.5)$$

Where, X1(t + 1) is the solution of the next iteration of t, $X_{best}(t)$ is the best obtained solution until t^{th} iteration, $X_M(t)$ is the locations mean value of the current solutions.

Narrowed Exploration

$$X_2(t+1) = X_{best}(t) \times Levy(D) + X_R(t) + (y-x) \times rand \qquad (3.6)$$

$$y = r \times cos\,\theta\,; \;\; x = r \times \sin\theta\;;\; r = r_1 + U \times D_1;\; \theta = -\omega \times D_1 + \theta_1$$

Here, $X_2(t+1)$ is the solution of the next iteration of t. x and y are used to present the spiral shape in search, Levy(D) denotes levy flight distribution function.

Expanded Exploitation

$$X_3(t+1) = \left(X_{best}(t) - X_M(t)\right) \times \alpha - rand + ((UB - LB) \times rand + LB) \times \delta \tag{3.7}$$

Here , $X_3(t+1)$ =solution of next iteration of t

X_{best} =approximate location of the prey until i^{th} iteration

$X_M(t)$ =mean value of the current solution at t^{th} iteration

Narrowed Exploitation

$$X_4(t+1) = QF \times X_{best}(t) - (G_1 \times X(t) \times rand) - G_2 \times Levy(D) + rand \tag{3.8}$$

$$QF(t) = t^{\frac{2 \times rand - 1}{(1-T)^2}}; \quad G_1 = 2 \times rand - 1; \; G_2 = 2 \times \left(1 - \frac{t}{T}\right)$$

Here, $X_4(t+1)$ denotes the solution of the next iteration of t, QF defines quality function, G1 denotes various motions of the AO and G2 denotes the flight slope of the AO.

Table 3.2 contains step by step instructions for coding AO

Table 3.2 : Pseudocode of Aquila Optimizer

```
Initialize the population X and algorithm parameters
while(The termination condition is not met) do
   Calculate the fitness function values
   Obtain Best Solutions based on fitness values
   for(i=1:N) do
      Update the values of X_M(t), x, y, G_1, G_2, Levy(d)
      if t ≤ (2/3) * T then
         if rand ≤ 0.5 then
            Update current solution using eqn.(3.5) [Expanded Exploration]
         else
```

Update current solution using eqn.(3.6) **[Narrowed Exploration]**
end if
else
if $rand \leq 0.5$ then
Update current solution using eqn.(3.7) **[Expanded Exploitation]**
else
Update current solution using eqn.(3.8) **[Narrowed Exploitation]**
end if
end if
end for
end while
return The best solution (X_{best})

3.3 Pelican Optimization Algorithm

The Pelican Optimization Algorithm (POA) is a nature-inspired optimization technique inspired by the foraging behavior of pelicans[99]. It mimics the cooperative hunting strategies of pelicans and their ability to adapt to dynamic environments. POA iteratively updates a population of candidate solutions, representing pelicans, to converge towards the optimal solution. It incorporates social interaction, individual learning, and global best information to strike a balance between exploration and exploitation[99].

The Pelican Optimization Algorithm has shown promising performance and has been applied to various optimization problems, including engineering design, image processing, and data clustering[99]. It provides a novel and effective approach to solving complex optimization problems.

Initially, population members are randomly initialized according to the lower bound and upper bound of the problem by following equation[100]

$$x_{i,j} = l_j + rand(u_j - l_j)\ where, i = 1, 2, \dots, N\ and\ j = 1, 2, \dots., m \quad (3.9)$$

The population matrix is used to identify the pelican population members in the proposed POA. Here, X is the population matrix of pelican and X_i is the ith pelican

$$X = \begin{bmatrix} X_1 \\ \vdots \\ X_i \\ \vdots \\ X_N \end{bmatrix}_{N\times m} = \begin{bmatrix} x_{1,1} & \cdots & x_{1,j} & \cdots & x_{1,m} \\ \vdots & \ddots & \vdots & \iddots & \vdots \\ x_{i,1} & \cdots & x_{i,j} & \cdots & x_{i,m} \\ \vdots & \iddots & \vdots & \ddots & \vdots \\ x_{N,1} & \cdots & x_{N,j} & \cdots & x_{N,m} \end{bmatrix}_{N\times m} \tag{3.10}$$

$$F = \begin{bmatrix} F_1 \\ \vdots \\ F_i \\ \vdots \\ F_N \end{bmatrix}_{N\times 1} = \begin{bmatrix} F(X_1) \\ \vdots \\ F(X_i) \\ \vdots \\ F(X_N) \end{bmatrix}_{N\times 1}$$

POA replicates pelican behavior and strategy when attacking and hunting prey in order to update candidate solutions.

Phase 1: Exploration Phase

$$x_{i,j}^{P_1} = \begin{cases} x_{i,j} + rand\left(p_j - I \cdot x_{i,j}\right), \ F_P < F_i; \\ x_{i,j} + rand\left(x_{i,j} - p_j\right), \ else \end{cases} ; \qquad X_i = \begin{cases} X_i^{P_1}, \ F_i^{P_1} < F_i ; \\ X_i \ , \ \ else \end{cases} \quad \begin{matrix} (3.11) \\ (3.12) \end{matrix}$$

Where $x_{i.j}^{P_1}$ is the new position of the ith pelican in the jth dimension. p_j is the location of prey in the jth dimension and F_p is the objective function. Here, $X_i^{P_1}$ is the new status of the ith pelican and $F_i^{P_1}$ is the objective function value based on phase 1.

Phase 2 : Exploitation Phase

$$x_{i,j}^{P_2} = x_{i,j} + R\left(1 - \frac{t}{T}\right)(2 \cdot rand - 1) \cdot x_{i,j} ; \qquad X_i = \begin{cases} X_i^{P_2}, & F_i^{P_2} < F_i \\ X_i , & else \end{cases} \quad \begin{matrix} (3.13) \\ (3.14) \end{matrix}$$

Here, in equation 3.13 & 3.14 $x_{i,j}^{P_2}$ is the updated position of the i^{th} pelican in j^{th} dimension and $F_i^{P_2}$ is the objective function value for $X_i^{P_2}$.

Table 3.3 contains step by step instructions for coding POA

Table 3.3 : Pseudocode of Pelican Optimization Algorithm

```
Initialize the pelican population with arbitrary placements and velocity
Evaluate the fitness of each pelican in the population
Set the current iteration count to 1

While the termination condition is not met:
   For each pelican in the population:
      Update the velocity of the pelican using the formula:
         velocity = (inertia weight) * velocity
            + (cognitive weight) * random() * (pelican's best position - current position)
            + (social weight) * random() * (global best position - current position)

      Update the position of the pelican using the formula:
         position = position + velocity
      Evaluate the fitness of the new position

      If the fitness of the new position is better than the fitness of the pelican:
         Update the pelican's best position and fitness

      If the fitness of the new position is better than the global best fitness:
         Update the global best position and fitness
   Increment the iteration count

   Update the termination condition (max. number of iterations or target fitness value)
Return the global best position and fitness
```

3.4 Dandelion Optimization Algorithm

The Dandelion Optimization Algorithm (DOA) is a nature-inspired optimization technique that mimics the seed dispersal process of dandelion plants[101, 102]. It aims to efficiently solve optimization problems by emulating the effective dispersal of dandelion seeds in the wind.

DOA updates a population of potential solutions, represented as dandelion seeds, in an iterative manner to find the optimal solution. Each seed adjusts its position based on its properties, interactions with neighboring seeds, and information from the best solution in the population.

To strike a balance between exploration and exploitation during optimization, DOA employs various strategies such as seed distribution, pollen competition, and seedling growth[103]. This approach has demonstrated outstanding performance in diverse fields, including engineering design, data clustering, and picture segmentation[104, 105].

DOA can be summarized as an optimization algorithm inspired by dandelion seed dispersal . It involves three stages in its operation[106].

Rising Stage

$$X_{t+1} = \begin{cases} X_t + \alpha \cdot v_x \cdot v_y \cdot lnY \cdot (X_s - X_t) & randn < 1.5 \\ X_t \cdot k & else \end{cases} \quad (3.15)$$

Here, X_{t+1} represents the position of the dandelion seed after t iteration and randn is the random number that follows the standard normal distribution.

Descending Stage

$$X_{t+1} = X_t - \alpha \cdot \beta_t \cdot \left(X_{mean_t} - \alpha \cdot \beta_t \cdot X_t\right) \ ; \ X_{mean_t} = \frac{1}{pop}\sum_{i=1}^{pop} X_i \quad (3.16)$$

This stage emphasizes the exploration, here X_{t+1} represents the position after j iteration and β_t denotes the Brownian motion, X_{mean_t} denotes the avg. position of the population.

Landing Stage

$$X_{t+1} = X_{elite} + levy(\lambda) \cdot \alpha \cdot (X_{elite} - X_t \cdot \delta) \quad (3.17)$$

This stage focuses on exploitation here X_{elite} denotes the optimal position of the dandelion in the i^{th} iteration and $levy(\lambda)$ represents the function of the levy flight.

Table 3.4 contains step by step instructions for coding DOA

Table 3.4 : Pseudocode of Dandelion Optimization Algorithm

```
Initialize the population of dandelions with random positions
Evaluate the fitness of each dandelion in the population
Initialize the global best position and fitness
Set the current iteration count to 1

While the termination condition is not met:
    For each dandelion in the population:
        For each neighbor of the dandelion:
            Generate a random direction vector
            Calculate the distance between the current dandelion and its neighbor
            Update the position of the neighbor dandelion using the formula:
                new_position = current_position + (random() * distance * direction_vector)

            Evaluate the fitness of the new position

            If the fitness of the new position is better than the fitness of the neighbor:
                Update the neighbor's position and fitness

        Update the best position and fitness of the current dandelion if necessary

    Update the global best position and fitness if necessary
    Increment the iteration count

    Update termination condition (max. number of iterations or target fitness value)

Return the global best position and fitness
```

3.5 Gazelle optimization algorithm

The Gazelle Optimization Algorithm (GOA) is a nature-inspired optimization technique that takes inspiration from the hunting behavior and agility of gazelles[107]. GOA aims to efficiently solve optimization problems by emulating the adaptive and swift movements of gazelles in search of food and evading predators.

GOA maintains a population of gazelles, where each gazelle represents a potential solution, and utilizes various strategies to update the population and search for the optimal solution[108, 109]. These strategies include individual movement, herd behavior, and predator-prey dynamics.

The individual movement of gazelles involves adjusting their positions based on their own attributes and information from the population's best solution. This allows for effective exploration of the search space[110, 111]. The herd behavior aspect of GOA emphasizes collaboration and communication among gazelles, facilitating information sharing and enhancing the overall search capability of the population[112]. It involves 2 stages in its operation

Exploitation

$$gazelle_{i+1} = gazlle_i + s.R * R_B *.(Elite_i - R_B *.gazelle_i) \qquad (3.18)$$

Here in equation 3.18 , $gazelle_{i+1}$ is the solution of the next iteration, $gazlle_i$ is the solution at the current iteration where s denotes the grazing speed.

Exploration

$$gazelle_{i+1} = \begin{cases} gazelle_i + CF[LB + R *.(UB - LB)] *.U & if\ r \le PSRs \\ gazelle_i + [PSRs(1-r) + r]\left(gazelle_{r_1} - gazelle_{r_2}\right) & else \end{cases} \qquad (3.19)$$

$$gazelle_{i+1} = gazelle_i + S \cdot \mu \cdot R *. R_L *. (Elite_i - R_L *. gazelle_i) \quad (3.20)$$

Here in equation 3.19 & 3.20 PSR is the predator success rate, CF is the cumulative effect of the predator.

Table 3.5 contains step by step instructions for coding GOA

Table 3.5 : Pseudocode of Gazelle Optimization Algorithm

Initialize all algorithm parameters
Initialize gazelle population
while current iteration is less than the max iteration
  Calculate the fitness value of the gazelles
  Construct the Elite gazelle matrix
  if r < 0.5
    Exploitation :
      Update gazelles based on equation (3.18)
  else
    Exploration :
      if $mod(iter, 2) == 0$
        $\mu = -1$
      else
        $\mu = 1$
      if $iter < size(gazelle, 1)/2$
        For the gazelle population $(i = 1, 2, \ldots, n/2)$
        Update gazelle based on the equation (3.20)
      else
        For the gazelle population $(i = n/2, \ldots, n)$
        Update gazelle based on the equation (3.20)
    end if
    Update the fitness and top-gazelle
    Apply PSRs effect and update based on the equation (3.19)
end while
return top-gazelle from the population

3.6 Zebra Optimization Algorithm

The Zebra Optimization Algorithm (ZOA) is a metaheuristic algorithm inspired by the natural behavior of zebras . It combines local search and global exploration to efficiently solve optimization problems. ZOA utilizes a population-based approach, with individuals representing potential solutions[113].

The Zebra Optimization Algorithm (ZOA) combines individual exploration, herd mobility, and information sharing to solve optimization problems efficiently[113]. It draws inspiration from the behavior of zebras, utilizing their natural tendencies to update positions and exchange ideas. ZOA has demonstrated promising results in various optimization domains, offering a novel approach inspired by nature[113]. ZOA utilizes two natural zebra behaviors to update its members, enhancing its performance[114] .

Foraging Behavior

$$x_{i,j}^{new,P1} = x_{i,j} + r \cdot \left(PZ_j - I \cdot x_{i,j}\right);\ \ X_i = \begin{cases} X_i^{new,P1}, & F_i^{new,P1} < F_i \\ X_i & else \end{cases} \quad \begin{matrix} (3.21) \\ (3.22) \end{matrix}$$

Here $X_i^{new,P1}$ is the new position of the i[th] zebra based on the first phase and $x_{i,j}^{new,P1}$ is the j[th] dimension value. $F_i^{new,P1}$is the objective function and PZ is the pioneer zebra which is the best member.

Defense Strategies Against Predators

$$x_{i,j}^{new,P2} = \begin{cases} S_1: x_{i,j} + R \cdot (2r-1) \cdot \left(1 - \frac{t}{T}\right) \cdot x_{i,j}, & P_s \leq 0.5 \\ S_2: x_{i,j} + r \cdot \left(AZ_j - I \cdot x_{i,j}\right), & else \end{cases} \quad (3.23)$$

$$X_i = \begin{cases} X_i^{new,P2}, & F_i^{new,P2} < F_i \\ X_i, & else \end{cases} \quad (3.24)$$

From equation 3.23 and 3.24 $X_i^{new,P2}$ is the new position of the ith zebra based on 2nd phase $x_{i,j}^{new,P2}$ is its jth dimension value and $F_i^{new,P2}$ is the objective function.

Table 3.6 contains step by step instructions for coding ZOA

Table 3.6 : Pseudocode of Zebra Optimization Algorithm

```
Initialization of optimization problem
Initialize all parameter, position and population
   Evaluate the objective function
   for t = 1:T
         Update pioneer zebra(PZ)
      for i = 1:N
         Phase 1 : Foraging behavior
            Determine the value of ith zebra using eqn.(3.21)
            Update ith zebra using eqn.(3.22)
         Phase 2: Defense Strategies Against Predators
            if Ps < 0.5, Ps = rand
               Determine the ith zebra's new status using mode S1 and the eqn 3.23
            else
               Determine the ith zebra's new status using mode S2 and the eqn 3.23
            end if
            Update the ith zebra using (3.24)
      end for i = 1:N
      Save the best solution
   end for t = 1:T
Return best solution obtained by ZOA
```

3.7 Osprey Optimization Algorithm

The Osprey Optimization Algorithm (OOA) is a nature-inspired optimization algorithm based on the hunting behavior of the osprey; a predatory bird recognized for its exceptional foraging ability. OOA uses the hunting behavior of ospreys to efficiently look for optimal solutions in difficult optimization issues.

To provide a robust and versatile optimization technique, this algorithm combines components of evolutionary computation and swarm intelligence[115]

Position Identification and Fish Hunting (Exploration)

$$x_{i,j}^{P1} = x_{i,j} + r_{i,j} \cdot \left(SF_{i,j} - I_{i,j} \cdot x_{i,j}\right) \tag{3.25}$$

$$x_{i,j}^{P1} = \begin{cases} x_{i,j}^{P1} & , lb_j \leq x_{i,j}^{P1} \leq ub_j \\ lb_j & , x_{i,j}^{P1} < lb_j \\ ub_j & , x_{i,j}^{P1} > ub_j \end{cases} \quad ; \quad X_i = \begin{cases} X_i^{P1} & , F_i^{P1} < F_i \\ X_i & , \quad else \end{cases} \qquad (3.26), (3.27)$$

Where X_i^{P1} is the new position of the ith osprey based on the 1st phase value, $x_{i,j}^{P1}$ is its jth dimension. F_i^{P1} is the objective function value and $SF_{i,j}$ is the selected fish for ith osprey in jth dimension.

Carrying The Fish to The Suitable Position (Exploitation)

$$x_{i,j}^{P2} = \begin{cases} x_{i,j}^{P2} & , lb_j \leq x_{i,j}^{P2} \leq ub_j \\ lb_j & , x_{i,j}^{P2} < lb_j \\ ub_j & , x_{i,j}^{P1} > ub_j \end{cases} \quad ; \quad X_i = \begin{cases} X_i^{P2} & , F_i^{P2} < F_i \\ X_i & , \quad else \end{cases} \qquad (3.28), (3.29)$$

Where X_i^{P1} is the new position of the ith osprey based on the 1st phase value, $x_{i,j}^{P1}$ is its jth dimension. F_i^{P1} is the objective function value and $SF_{i,j}$ is the selected fish for ith osprey in jth dimension.

Table 3.7 : Pseudocode of Osprey Optimization Algorithm

```
Initialize problem information
Initialize OOA population and parameters
   Evaluate the objective function
   for t = 1:T
      for i = 1:N
         Phase 1: Exploration
            Update fish position set
```

```
            Calculate new position
            Check the boundary conditions for the new position using eqn.(3.26)
            Update ith member using eqn.(3.27)
        Phase 2 : Exploitation
            Calculate new position
            Check the boundary conditions for the new position using eqn.(3.28)
            Update ith member using eqn.(3.29)
    end for i = 1:N
  end for t = 1:T
return best candidate solution
```

3.8 Summary

This chapter focused on various optimization algorithms, providing an overview of their principles and illustrating their flowcharts. We explored multiple algorithms, outlining their key characteristics and depicting their step-by-step processes through flowcharts. By delving into these optimization methods, we gained a comprehensive understanding of their workings and how they can be applied in practice.

Chapter 4
Results And Analysis

This chapter implements algorithms from Chapter 3 to evaluate their effectiveness and reliability. A comparative analysis explores their strengths, limitations, and practical applications, providing valuable insights.

4.1 Load Profile

In order to apply the optimization algorithms, load data is necessary. The study utilized load data from the Islamic University of Technology (IUT), along with solar radiation and wind speed measurements, to model the hourly load demands using a random Gaussian distribution. A graphical representation of the typical day's load demand for IUT is shown in Figure 4.1.

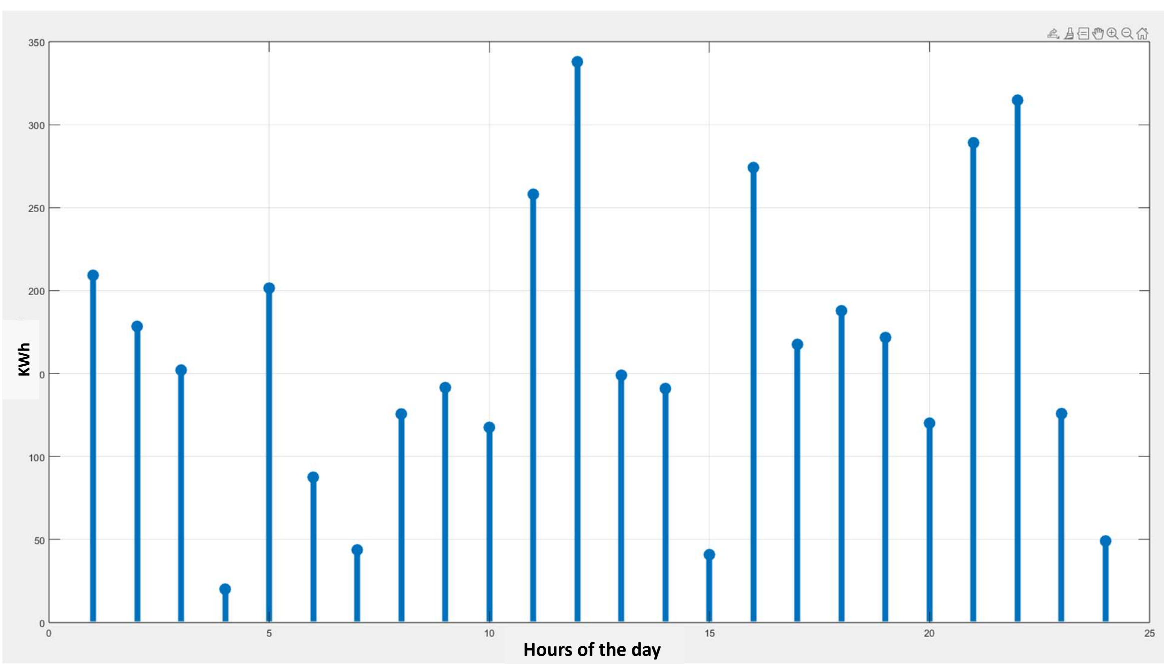

Fig. 4.1: Hourly Load Data (for a day)

4.2 Simulation environment

We used MATLAB (2023) to run our simulations, as this is a simulation- based research there were no hardware and machineries involved. The workload totaled 8760 hours over the course of a year. In each iteration the hourly data of solar irradiance, wind velocity, load demand and the daily data of food waste was given as input. The algorithm was simulated 30 times in a row, independently. Each of these 30 distinct runs consisted of 300 iterations with a population of 150 to ensure a complete execution of the algorithm. The algorithms employed in this study cease their execution when the maximum iteration limit is attained. The result of the iterations gives the best values of the optimization parameters $N_{WG}, N_{PV}, N_{bio}, N_{bat}, h$ and β maintaining their individual constraints has we have discussed in chapter 2. The optimized values of each parameter are used in the objective function to find the best overall cost .

4.3 Obtained Results

After performing 30 independent runs with 300 iterations each, we observed that the optimization algorithm reached an equilibrium state. To assess the convergence of the algorithm, we plotted the convergence curve using the best cost as the convergence metric. The convergence curve illustrates the relationship between the number of iterations and the best cost achieved by the algorithm. It serves as a valuable tool for analyzing the algorithm's performance and evaluating its progress towards finding the optimal solution. By examining the convergence curve, we can gain insights into the algorithm's convergence behavior, such as whether it converges smoothly, reaches a stable state, or experiences fluctuations or plateaus throughout the iterations.

Fig 4.2 to Fig 4.8 represents convergence curves of the used algorithms

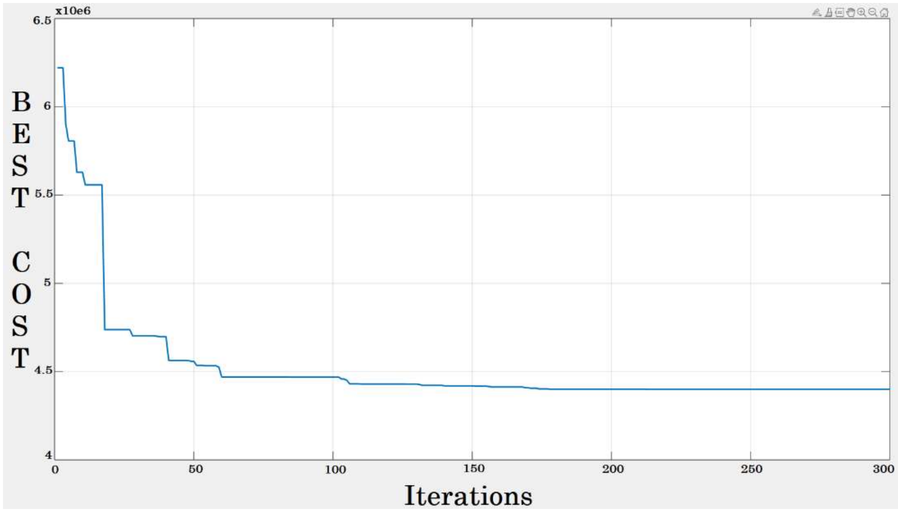

Fig 4.2: Convergence curve of PSO **X-axis :** iterations; **Y-axis :** best cost

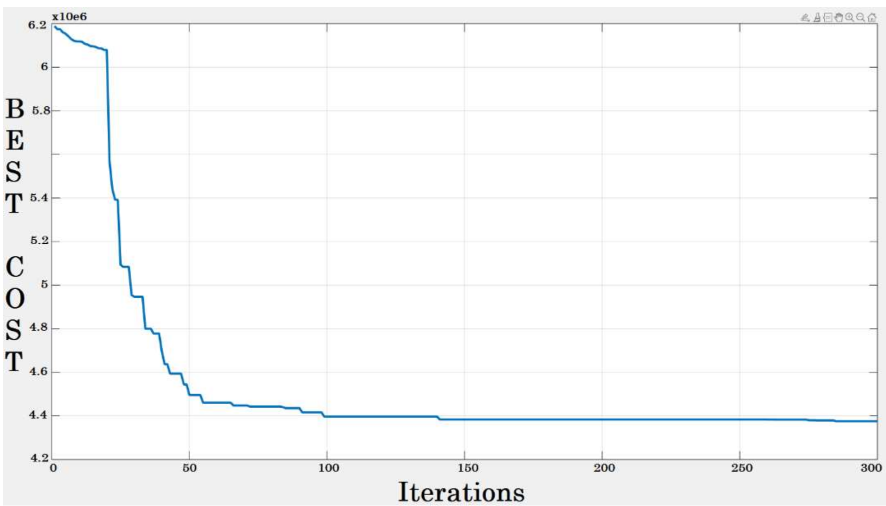

Fig 4.3: Convergence curve of AO; **X-axis :** iterations; **Y-axis :** best cost

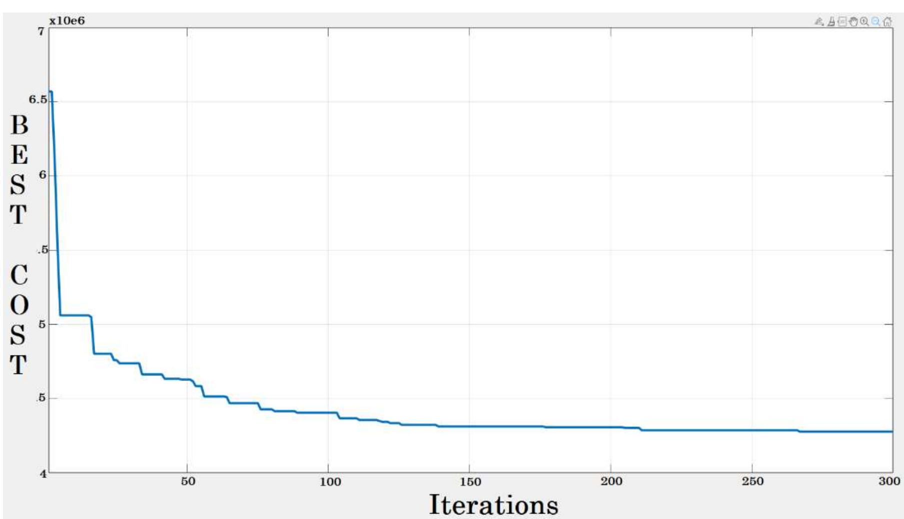

Fig 4.4: Convergence curve of POA; **X-axis :** iterations; **Y-axis :** best cost

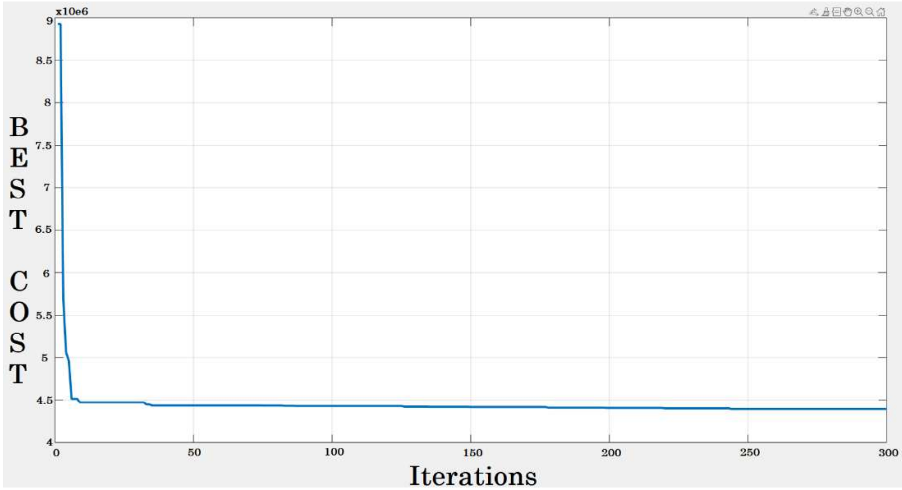

Fig 4.5: Convergence curve of DOA; **X-axis :** iterations; **Y-axis :** best cost

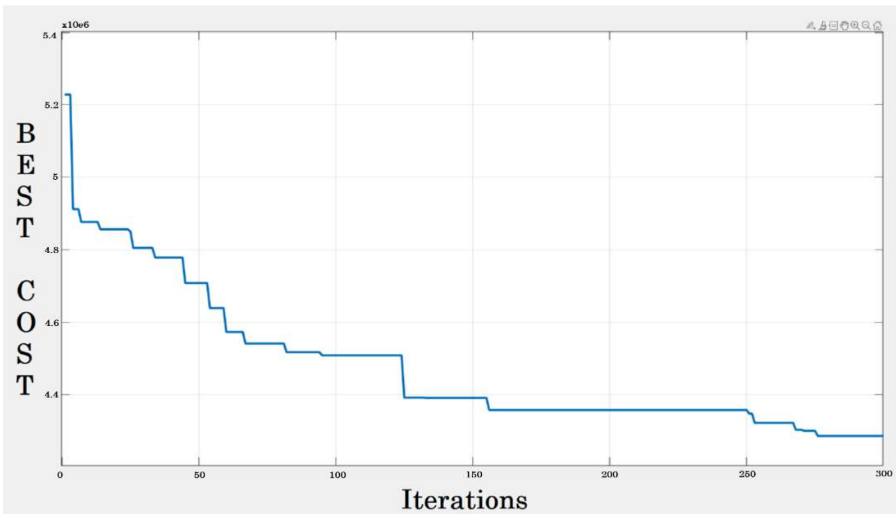

Fig 4.6: Convergence curve of GOA; **X-axis :** iterations; **Y-axis :** best cost

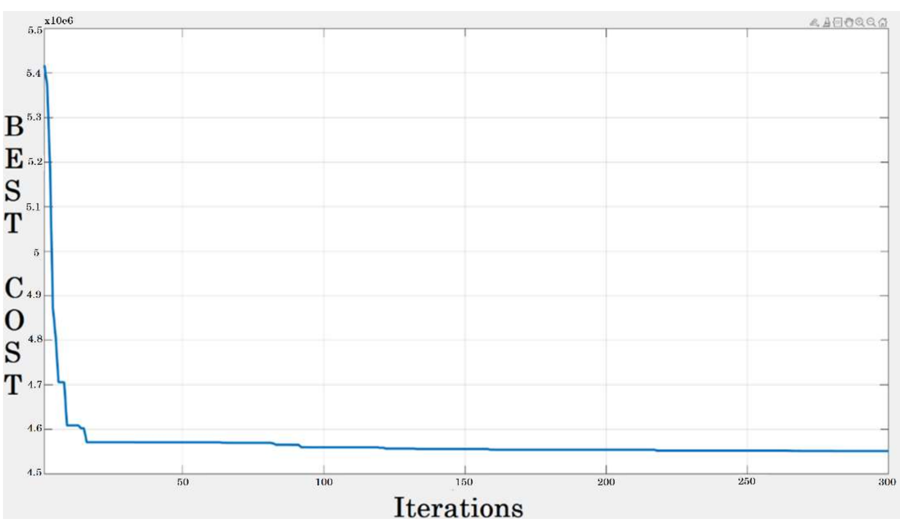

Fig 4.7: Convergence curve of ZOA; **X-axis :** iterations; **Y-axis :** best cost

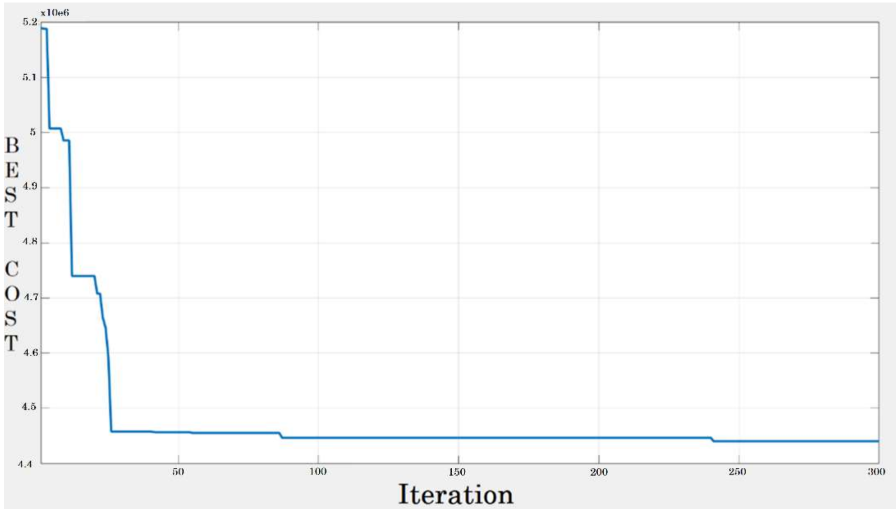

Fig 4.8: Convergence curve of OOA; **X-axis :** iterations**; Y-axis :** best cost

The obtained data for all the optimization algorithm are presented in table 4.1

Table 4.1 : Optimized Cost and Parameter results

No.	**Optimization Algorithm**	**Best Cost $**	N_{wg}	N_{pv}	N_{bat}	β	**h**	N_{bio_eng}
1.	**PSO**	4399402.5	15	125	3427	18	22	6
2.	**AO**	4375318.69	14	168	3381	13.1	16	10
3.	**POA**	4276504.73	19	69	3343	31.4	11.3	9
4.	**DOA**	4394996.11	18	267	3338	8.2	12.4	8
5.	**GOA**	4284792.80	19	46	3362	51.6	12.6	10
6.	**ZOA**	4551329.74	12	159	3547	14.4	13	3
7.	**OOA**	4440412	63	79	3367	23.6	14.7	5

In this study, we conducted a comprehensive comparison of six optimization algorithms for our HRES model : Particle Swarm Optimization (PSO), Aquila Optimizer (AO), Pelican Optimization Algorithm (POA), Dandelion Optimizing), Gazelle Optimization Algorithm (GOA), Zebra Optimization Algorithm (ZOA), and Osprey Optimization Algorithm (OOA).

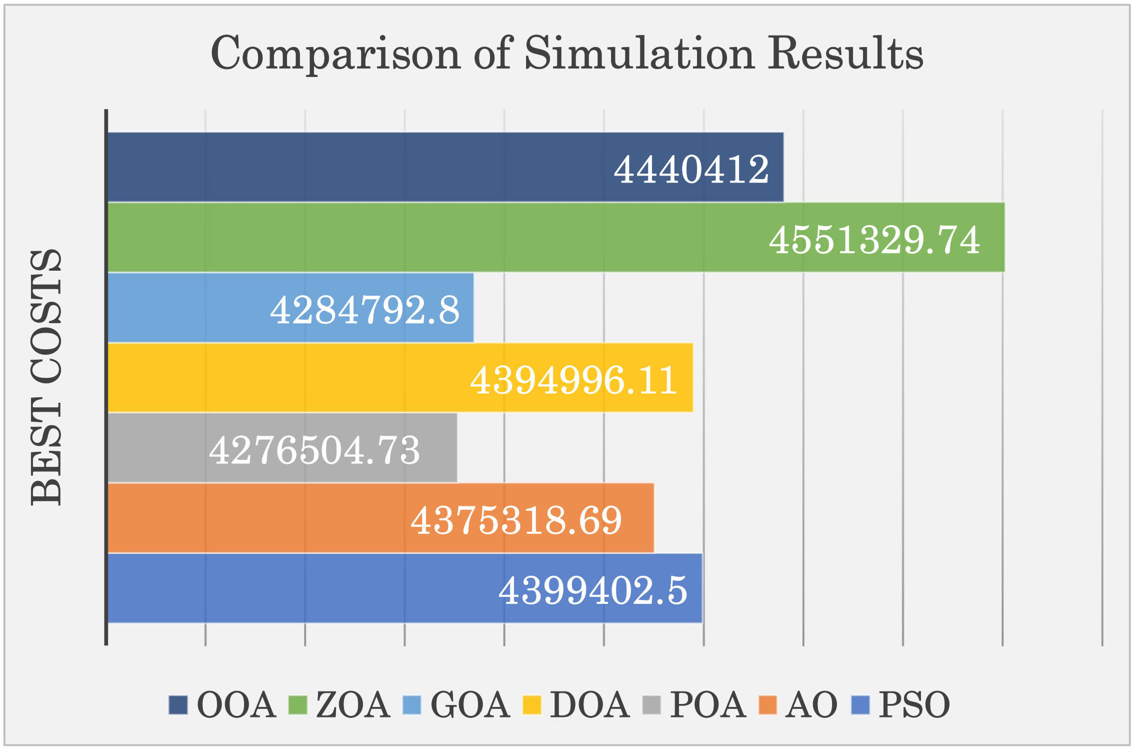

Fig 4.9 : Comparison of Algorithm by simulated result

The primary objective of this study was to identify the most effective optimization algorithm that can achieve the lowest best cost while utilizing limited resources and minimizing expenses. A lower best cost indicates a better optimization algorithm. Analyzing table 4.1 and Fig 4.9 it can be said that Pelican Optimization Algorithm (POA) exhibited the lowest best cost of 4276504.73$.

This indicates that POA outperformed the other algorithms in terms of achieving the desired optimization goal while utilizing limited resources and minimizing expenses. The POA algorithm demonstrated superior efficiency in finding the optimal solution, resulting in lower costs compared to other algorithms.

4.4 Performance Comparison

In order to determine the relative performance of each optimization algorithm, we calculate the percentage difference between each algorithm's best cost and the lowest best cost observed among all algorithms which is presented in Table 4.2.

Table 4.2 : Performance Comparison of Algorithms

Optimization Algorithm	Best Cost($)	Percentage Difference
Particle Swarm Optimization	4399402.5	2.87%
Aquila Optimizer	4375318.69	2.31%
Pelican Optimization Algorithm	4276504.73	0%
Dandelion Optimizing Algorithm	4394996.11	2.76%
Gazelle Optimization Algorithm	4284792.80	0.19%
Zebra Optimization Algorithm	4551329.74	6.43%
Osprey Optimization Algorithm	4440412	3.85%

Based on the calculated percentage differences, we can analyze the performance of each optimization algorithm:

The Pelican Optimization Algorithm (POA) and the Gazelle Optimization Algorithm (GOA) have the lowest percentage differences of 0% and 0.19% respectively, indicating that they perform almost as well as the algorithm with the lowest best cost (POA).

The Aquila Optimizer (AO) and the Dandelion Optimizing Algorithm (DOA) exhibit slightly higher percentage differences of 2.31% and 2.76% respectively. Although these algorithms are not as efficient as the lowest cost algorithm, they still demonstrate competitive performance.

The Particle Swarm Optimization (PSO) algorithm and the Osprey Optimization Algorithm (OOA) have percentage differences of 2.87% and 3.85%

respectively. While they are less efficient than the algorithms with lower percentage differences, they still offer considerable optimization capabilities.

The Zebra Optimization Algorithm (ZOA) exhibits the highest percentage difference of 6.43%. This indicates that it is the least efficient algorithm in terms of minimizing the best cost.

In summary, based on the comparison of the best costs, the optimization algorithms can be ranked as follows: POA and GOA exhibited the lowest best costs, followed by AO, DOA, PSO, OOA, and ZOA. Therefore, if the primary goal is to utilize limited resources while minimizing expenses, POA and GOA are the recommended optimization algorithms due to their superior performance. However, it is important to consider other factors such as convergence speed, robustness, and the specific requirements of the problem at hand before finalizing the choice of an optimization algorithm.

To assess the feasibility of the optimized model, we'll analyze how long it will take for the plant to become profitable by reducing the current annual electricity bill of $207,301.23 at the Islamic University of Technology (IUT).

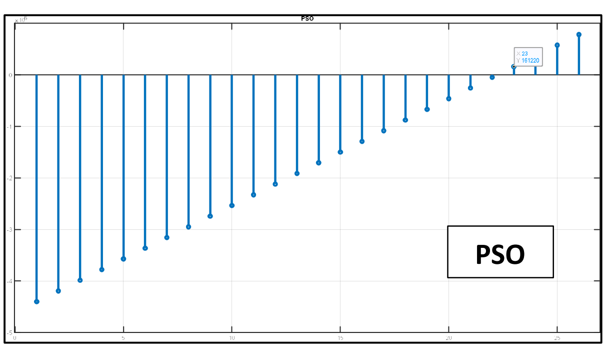

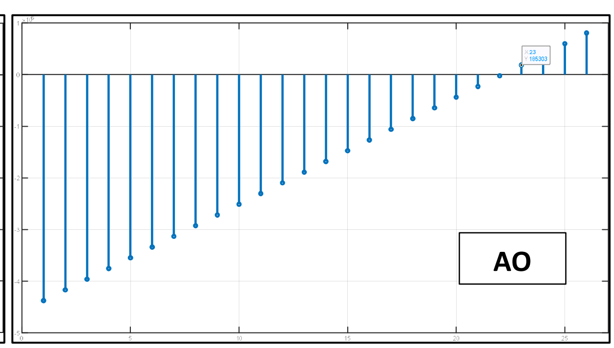

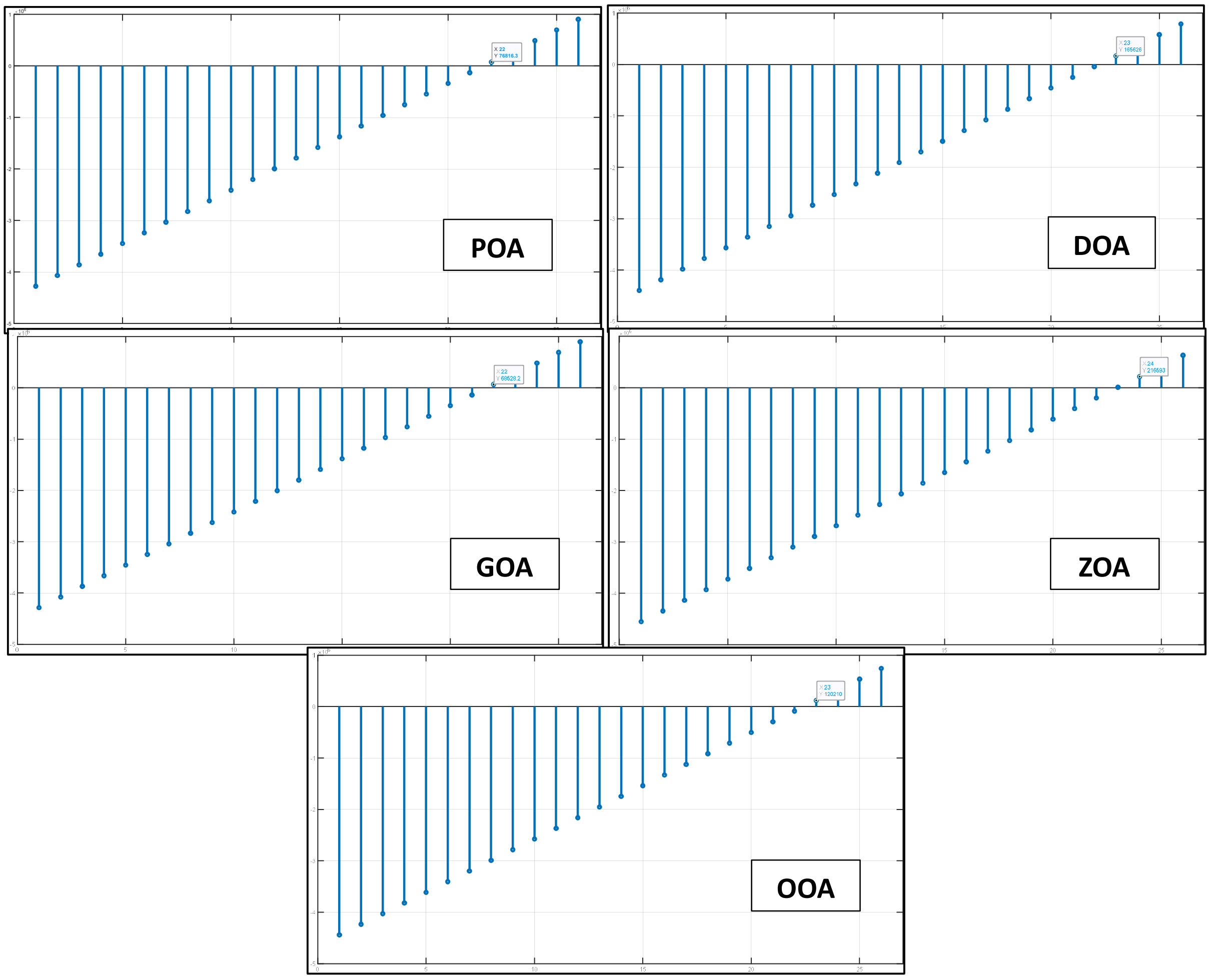

Fig 4.10 : Profitability timeframes of different algorithm

By investing in the most cost-effective solution, we can calculate the time it will take for the plant to reach a point where the savings on the annual electric bill outweigh the initial investment cost. We will compare the profitability timeframes for different algorithms.

From Fig 4.10 it can be said that POA becomes profitable after 20 years 7months which about 1 month earlier than GOA. In table 4.3 time required for an algorithm to become profitable is listed.

Table 4.3 : Feasibility Comparison of Algorithms

Optimization Algorithm	Period Required to Be Profitable
Particle Swarm Optimization	21years 2months 12days
Aquila Optimizer	21years 1months 9days
Pelican Optimization Algorithm	20years 7months 16days
Dandelion Optimizing Algorithm	21years 2months 13days
Gazelle Optimization Algorithm	20years 8months 1day
Zebra Optimization Algorithm	21years 11months 16days
Osprey Optimization Algorithm	21years 5months 1day

4.5 Summary

In this chapter, we conducted comprehensive testing and analysis of all the algorithms. We examined each algorithm's performance and presented a detailed evaluation. Additionally, we determined the timeframe for the plant to become profitable by considering the cost savings achieved through these algorithms.

Chapter 5

Conclusions and Prospects for Future Research

5.1 Conclusion

Chapter 1 provides a comprehensive overview of the energy crisis and the need for alternative energy sources. It conducts a detailed literature review on Hybrid Renewable Energy Systems (HRES) and single objective optimization (SOO), emphasizing their importance in addressing the energy crisis and achieving sustainable energy solutions. The chapter concludes by outlining the thesis objectives and presenting the organization of the subsequent chapters. Overall, Chapter 1 serves as a foundational introduction to the research on HRES optimization and its contribution to resolving the energy crisis.

Chapter 2 delves into the mathematical modeling of the proposed Hybrid Renewable Energy System (HRES). Each component, including PV, wind turbines, biogas, and batteries, is thoroughly explored with detailed sections containing equations, costs, and specifications. The chapter introduces objective functions to minimize the HRES cost over 25 years and evaluates system reliability through Loss of Power Supply Probability (LPSP). The optimization methodology, tailored to the complexity of the problem, aims to determine the best configuration and operation strategy by considering objectives, constraints, and system dynamics. These mathematical models, objective functions, and optimization approaches set the stage for subsequent chapters, where optimization techniques will be implemented to evaluate the performance of the HRES.

In Chapter 3, various popular metaheuristic algorithms, namely Particle Swarm Optimization (PSO), Aquila Optimizer (AO), Pelican Optimization Algorithm

(POA), Dandelion Optimizing Algorithm (DOA), Gazelle Optimization Algorithm (GOA), Zebra Optimization Algorithm (ZOA), and Osprey Optimization Algorithm (OOA), are explored. The discussion includes the formulation of mathematical models and the presentation of pseudocodes for each of these algorithms. By providing mathematical models and pseudocodes, Chapter 3 offers a comprehensive understanding of the workings and implementation of these metaheuristic algorithms.

Chapter 4 provides a detailed analysis of the simulation results obtained from the proposed HRES model. It covers an overview of the load profile, convergence curves, and the use of MATLAB for data analysis and graph plotting. The chapter includes a constructive comparison of the algorithms discussed in Chapter 3, evaluating their performance in optimizing the HRES model. Additionally, it explores the profitability of the HRES plant with the examined algorithms. Overall, Chapter 4 offers valuable insights into the simulation results, algorithm effectiveness, and the financial viability of the proposed HRES model.

In this study, we compared seven optimization algorithms for an HRES model to minimize costs. The Pelican Optimization Algorithm (POA) emerged as the most cost-effective, surpassing the other algorithms. The Gazelle Optimization Algorithm (GOA) also demonstrated strong performance. Consequently, we recommend using either POA or GOA. Based on profitability analysis, POA becomes profitable in approximately 20 years and 7 months, slightly ahead of GOA.

5.2 Prospects for Future Research

The thesis focused on offline analysis using recorded load data. Future research can improve the analysis by incorporating real-time load profiles and considering weather uncertainties for PV modules, biogas models, and wind turbine models.

These enhancements will lead to more accurate and reliable analyses of hybrid renewable energy systems.

Furthermore, while the current work employed a single objective optimization (SOO) approach, future studies could explore the benefits of utilizing multi-objective optimization (MOO) techniques. MOO has the potential to provide superior performance by simultaneously considering multiple objectives and generating a range of Pareto-optimal solutions.

The research in this thesis primarily utilized software simulations. To enhance the practicality and reliability of the proposed models, future research can explore the implementation of hardware models. By transforming the proposed system into a miniature form, the effectiveness and feasibility of the models can be further evaluated.

References

[1] BP, "www.bp.com," ed: BP.
[2] I. E. Agency, "https://www.iea.org/," ed.
[3] "Global Footprint Network,"" https://www.footprintnetwork.org/our-work/ecological-footprint/" ed.
[4] "The World Counts,"" https://www.theworldcounts.com/economies/global/effects-of-consumerism" ed.
[5] "Ember,"" https://ember-climate.org/data-catalogue/yearly-electricity-data/ " ed.
[6] "National Oceanic and Atmospheric Administration,"" https://www.ncdc.noaa.gov/sotc/global/202013" ed.
[7] S. R. Ahmed, "Unlocking the planet-saving power of alternative energy." [Online]. Available: https://www.tbsnews.net/features/panorama/unlocking-planet-saving-power-alternative-energy-586398
[8] "United Nations,"" https://www.un.org/en/climatechange/raising-ambition/renewable-energy" ed.
[9] "Inspire Clean Energy,"" https://www.inspirecleanenergy.com/blog/clean-energy-101/what-is-sustainable-energy" ed.
[10] T. Adrian, P. Bolton, and A. M. Kleinnijenhuis, "IMF Blog." [Online]. Available: https://www.imf.org/en/Blogs/Articles/2022/06/08/how-replacing-coal-with-renewable-energy-could-pay-for-itself
[11] IRENA. (2022, July 13) Renewable Power Remains Cost-Competitive amid Fossil Fuel Crisis. *International Renewable Energy*.
[12] "Efficiency Is The Most Cost-Effective Pathway To Reliable Renewables," ALLIANCE TO SAVE ENERGY'S BLOG, Washington, 2022.
[13] H. Ritchie, M. Roser, and P. Rosado, "CO_2 and Greenhouse Gas Emissions," Our World in Data, 2020.
[14] IEA, "CO2 Emissions in 2022," www.iea.org, 2023.
[15] "Benefits of Renewable Energy Use." [Online]. Available: https://www.ucsusa.org/resources/benefits-renewable-energy-use
[16] H. Lund, "Renewable energy strategies for sustainable development," *Energy,* vol. 32, no. 6, pp. 912-919, 2007.
[17] R. Ramakumar, "Renewable Energy Sources and Developing Countries," *IEEE Transactions on Power Apparatus and Systems,* vol. PAS-102, no. 2, pp. 502 - 510, 1983.
[18] S. R. Bull, "Renewable energy today and tomorrow," *Proceedings of the IEEE,* vol. 89, no. 8, pp. 1216-1226, 2001.
[19] C. E. a. G. Ozkaya, "Turkey's 2023 Energy Strategies and Investment Opportunities for Renewable Energy Sources: Site Selection Based on ELECTRE," *Sustainability,* vol. 11, no. 7, p. 2136, 2019.
[20] T. Ise, M. Kita, and A. Taguchi, "A Hybrid Energy Storage With a SMES and Secondary Battery," *IEEE Transactions on Applied Superconductivity,* vol. 15, no. 2, pp. 1915 - 1918, 2005.
[21] H. F. F. M. He, K. Yahya, M. Mohamed, I. Alhamrouni, and L. J. Awalin, "Optimal Design of Hybrid Renewable Systems, Including Grid, PV, Bio Generator, Diesel Generator, and Battery," *Sustainability,* vol. 15, no. 4, p. 3297, 2023.
[22] P. K. Sharma, Mohan & Sharma, Arvind, "Economic Analysis of a Building Integrated Photovoltaic System Without and With Energy Storage Economic Analysis of a Building Integrated Photovoltaic System Without and With Energy Storage," in *HEREM 2019 IOP Conf. Series: Materials Science and Engineering605 (2019) 012013 IOP Publishing*, 2019.
[23] S. S. Krishnamoorthy Murugaperumal, G.R.K.D. Satya Prasad, "Optimum design of hybrid renewable energy system through load forecasting and different operating strategies for rural electrification," *Sustainable Energy Technologies and Assessments,* vol. 37, p. 100613, 2020.

[24] F. Yilmaz, "Development and modeling of the geothermal energy based multigeneration plant for beneficial outputs: Thermo-economic and environmental analysis approach," *Renewable Energy,* vol. 189, pp. 1074-1085, 2022.

[25] A. A. H. El-houari, S. Rehman, M.S. Buker, T. Kousksou, A. Jamil, B. El Amrani, "Feasibility evaluation of a hybrid renewable power generation system for sustainable electricity supply in a Moroccan remote site," *Journal of Cleaner Production,* vol. 277, p. 123534, 2020.

[26] F. P. Akbar Maleki, "Optimal sizing of autonomous hybrid photovoltaic/wind/battery power system with LPSP technology by using evolutionary algorithms," *Solar Energy,* vol. 115, pp. 471-483, 2015.

[27] S. Sanajaoba, & Fernandez, "Maiden application of Cuckoo Search algorithm for optimal sizing of a remote hybrid renewable energy System," *Renewable energy,* vol. 96, pp. 1-10, 2016.

[28] A. Kamjoo, Alireza Maheri, Arash M. Dizqah, and Ghanim A. Putrus, "Multi-objective design under uncertainties of hybrid renewable energy system using NSGA-II and chance constrained programming," *International journal of electrical power & energy systems,* vol. 74, pp. 187-194, 2016.

[29] A. S. O. Ogunjuyigbe, T. R. Ayodele, and O. A. Akinola, "Optimal allocation and sizing of PV/Wind/Split-diesel/Battery hybrid energy system for minimizing life cycle cost, carbon emission and dump energy of remote residential building," *Applied Energy,* vol. 171, pp. 153-171, 2016.

[30] P. Paliwal, N. P. Patidar, and R. K. Nema, "Determination of reliability constrained optimal resource mix for an autonomous hybrid power system using Particle Swarm Optimization," *Renewable energy,* vol. 63, pp. 194-204, 2014.

[31] J.-C. T. K. Shivam, and S.-C. Wu, "Multi-Objective Sizing Optimization of a Grid-Connected Solar–Wind Hybrid System Using Climate Classification: A Case Study of Four Locations in Southern Taiwan," *Energies,* vol. 13, no. 10, p. 2505, 2020.

[32] J. Zhao, Yuan, X., "Multi-objective optimization of stand-alone hybrid PV-wind-diesel-battery system using improved fruit fly optimization algorithm," *Soft Comput,* vol. 20, pp. 2841–2853, 2016.

[33] T. F. Agajie, Ali, A., Fopah-Lele, A., Amoussou, I., Khan, B., Velasco, C.L.R., & Tanyi, E, "Optimal Sizing of Hybrid Renewable Energy Sources Systems," *Encyclopedia,* 2023.

[34] R. N. P. Shebaz A. Memon, "An overview of optimization techniques used for sizing of hybrid renewable energy systems," *Renewable Energy Focus,* vol. 39, pp. 1-26, 2021.

[35] S. Kumar, Sharma, S., Sood, Y.R. et al, "A Review on different Parametric Aspects and Sizing Methodologies of Hybrid Renewable Energy System," *J. Inst. Eng. India Ser. B,* vol. 103, pp. 1345–1354, 2022.

[36] B. S. B. a. Z. M. Salameh, "Methodology for optimally sizing the combination of a battery bank and PV array in a wind/PV hybrid system," *in IEEE Transactions on Energy Conversion,* vol. 11, no. 2, pp. 367-375, 1996.

[37] A. Mahmoudi, Javed, S.A, "Probabilistic Approach to Multi-Stage Supplier Evaluation: Confidence Level Measurement in Ordinal Priority Approach," *Group Decis Negot,* vol. 31, pp. 1051–1096, 2022.

[38] J. Smith, Johnson, A., Brown, K, "The role of energy storage systems in mitigating the intermittency of renewable energy sources," *Renewable Energy Journal,* vol. 45, no. 3, pp. 189-205, 2022.

[39] L. L. Hongxing Yang, Wei Zhou, "A novel optimization sizing model for hybrid solar-wind power generation system," *Solar Energy,* vol. 81, no. 1, pp. 76-84, 2007.

[40] M. H. N. W. D. Kellogg, G. Venkataramanan and V. Gerez, "Generation unit sizing and cost analysis for stand-alone wind, photovoltaic, and hybrid wind/PV systems," *in IEEE Transactions on Energy Conversion,* vol. 13, no. 1, pp. 70-75, 1998.

[41] Y. González Cusa, Moya Rodríguez, J. L. ., Vieira de Melo, S. A. B. ., & Andrade Torres, E., "Optimization of Hybrid Renewable Energy Systems for Power Generation: A Bibliometric Review," *International Journal for Innovation Education and Research,* vol. 9, no. 3, pp. 369–393, 2021.

[42] R. A. G. Rajesh Kumar, Ajay Kumar Bansal, "Economic analysis and power management of a stand-alone wind/photovoltaic hybrid energy system using biogeography based optimization algorithm," *Swarm and Evolutionary Computation,* vol. 8, pp. 33-43, 2013.

[43] S. Lee, Kim, J., Park, H, "Hybrid solutions for multi-objective optimization," *A review. Journal of Optimization,* vol. 36, no. 2, pp. 125-142, 2021.

[44] M. G. A. Arabali, M. Etezadi-Amoli and M. S. Fadali, "Stochastic Performance Assessment and Sizing for a Hybrid Power System of Solar/Wind/Energy Storage," *in IEEE Transactions on Sustainable Energy,* vol. 5, no. 2, pp. 363-371, 2014.

[45] S. Ahmed, Zhang, G., Ahmad, S., Akhtar, N, "Stochastic evaluation of intermittent PV and wind power generating systems using ARMA models," *Renewable Energy,* vol. 78, pp. 535-545, 2019.

[46] Y. Liu, Chen, C., Li, Z., Li, M., Zhang, B, "Stochastic Evaluation of Intermittent Renewable Power Generation Based on ARMA Model," *International Journal of Electrical Power & Energy Systems,* vol. 95, pp. 194-199, 2018.

[47] L. Zhang, Wang, C., Zhang, W., Fu, Y., Zhang, L, "Hybridization of Pattern Search and Sequential Monte Carlo Simulation for Optimal Sizing of Microgrids," *Energies,* vol. 13, no. 5, p. 1204, 2020.

[48] T. Nguyen, Tran, D., Phan, L., Le, H., Nguyen, H, "A Hybrid Model for Microgrid Design in Rural and Isolated Areas," *Energies,* vol. 13, no. 15, p. 3998, 2020.

[49] M. Li, Zhang, Y., Wang, C., Zhang, P., & Zeng, P, "Hybrid Pattern Search and Sequential Monte Carlo Simulation for Optimal Microgrid Sizing in Rural and Isolated Areas," *IEEE Transactions on Sustainable Energy,* vol. 11, no. 2, pp. 1114-1126, 2020.

[50] S. R. P. B. Bhandari, K.-T. Lee, and S.-H. Ahn, "Mathematical modeling of hybrid renewable energy system: A review on small hydro-solar-wind power generation," *international journal of precision engineering and manufacturing-green technology,* vol. 1, pp. 157-173, 2014.

[51] O. E. a. M. Uzunoglu, "Optimum design of hybrid renewable energy systems: Overview of different approaches," *Renewable and Sustainable Energy Reviews,* vol. 16, pp. 1412-1425, 2012.

[52] S. S. C. Sunanda Sinha, "Review of software tools for hybrid renewable energy systems," *Renewable and Sustainable Energy Reviews,* vol. 32, pp. 192-205, 2014.

[53] S. K. N. a. H. R. Ghosh, "Techno-economical analysis of off-grid hybrid systems at Kutubdia Island, Bangladesh," *Energy Policy,* vol. 38, pp. 976-980, 2010.

[54] P. N. J. A. M. Haidar, and M. Shawal, "Optimal configuration assessment of renewable energy in Malaysia," *Renewable Energy,* vol. 36, pp. 881-888, 2011.

[55] T. M. W. a. A. Ilinca, "The utility of energy storage to improve the economics of wind–diesel power plants in Canada," *Renewable energy,* vol. 33, pp. 1544-1557, 2008.

[56] H. A. K. M. T. Chaichan, A. M. Mahdy, and A. A. Al-Waeely, "Optimal sizing of a hybrid system of renewable energy for lighting street in Salalah-Oman using," *International Journal of Scientific Engineering and Applied Science (IJSEAS),* vol. 2, pp. 157-164, 2016.

[57] J. L. B.-A. R. Dufo-López, and F. Mendoza, "Design and economical analysis of hybrid PV–wind systems connected to the grid for the intermittent production of hydrogen," *Energy Policy,* vol. 37, pp. 3082-3095, 2009.

[58] L. P. Kaelbling, Littman, M. L., & Moore, A. W, "Reinforcement learning: A survey," *Journal of artificial intelligence research,* vol. 4, pp. 237-285, 1996.

[59] S. Saha, Sarker, R. A., & Essam, D. L, "Single-objective optimization algorithms," in *In Optimization in Practice with MATLAB®*: CRC Press, 2017, pp. 191-205.

[60] K. Z. a. R. Laur, "Constrained Single-Objective Optimization Using Differential Evolution," in *006 IEEE International Conference on Evolutionary Computation*, Vancouver, BC, Canada, 2006, pp. 223-230.

[61] R. Storn, & Price, K., "Differential evolution – A simple and efficient heuristic for global optimization over continuous spaces," *Journal of Global Optimization,* vol. 11, no. 4, pp. 341-359, 1997.

[62] T. T. Nguyen, "A high performance social spider optimization algorithm for optimal power flow solution with single objective optimization," *Energy,* vol. 171, pp. 218-240, 2019.

[63] S. Kumar, & Padhy, N. P., "Novel Improved Social Spider Optimization Method for Multi-Objective Optimal Power Flow," *International Journal of Electrical Power & Energy Systems,* vol. 122, p. 106042, 2020.

[64] L. Hu, Li, J., Liu, Y., & Zhang, Q., "A Novel Improved Social Spider Optimization for Optimum Power Flow," *Energies,* vol. 14, no. 7, p. 1803, 2021.

[65] J. Zhou, Wang, J., Li, Y., & Wang, C., "Novel Improved Social Spider Optimization for Optimal Power Flow with Multiple Objectives," *Energies,* vol. 15, no. 1, p. 50, 2022.

[66] E. Koutroulis, Dionissia Kolokotsa, Antonis Potirakis, and Kostas Kalaitzakis, "Methodology for optimal sizing of stand-alone photovoltaic/wind-generator systems using genetic algorithms," *Solar energy,* vol. 80, no. 9, pp. 1072-1088, 2006.

[67] M. L. Kolhe, & Kolhe, S., "Optimal sizing of stand-alone photovoltaic/wind hybrid energy systems," *Solar Energy,* vol. 72, no. 3, pp. 235-245, 2002.

[68] C. R. Lopez, de Sousa, R. R., & Ferreira, J. A., "Stand-alone Photovoltaic/Wind Generator Systems Sizing Methodology Optimization," *In IEEE Latin America Transactions,* vol. 13, no. 3, pp. 879-886, 2015.

[69] D. K. E. Koutroulis, A. Potirakis, and K. Kalaitzakis, "Methodology for optimal sizing of stand-alone photovoltaic/wind-generator systems using genetic algorithms," *Solar energy,* vol. 80, pp. 1072-1088, 2006.

[70] A. A. I. Tégani, M.Y. Ayad, M. Becherif, R. Saadi, O. Kraa, "Optimal Sizing Design and Energy Management of Stand-alone Photovoltaic/Wind Generator Systems," *Energy Procedia,* vol. 50, pp. 163-170, 2014.

[71] A. Boulkroune, Rekioua, D., & Bachir, G., "Optimal Sizing and Strategy Control of a Stand-Alone Hybrid Power System Using Differential Flatness Approach," *IEEE Transactions on Energy Conversion,* vol. 33, no. 2, pp. 636-647, 2018.

[72] S. G. Y. Sawle, and A. K. Bohre, "Review of hybrid renewable energy systems with comparative analysis of off-grid hybrid system," *Renewable and Sustainable Energy Reviews,* vol. 81, pp. 2217-2235, 2018.

[73] S. J. M. D. Al-Falahi, and H. Enshaei, "A review on recent size optimization methodologies for standalone solar and wind hybrid renewable energy system," *Energy Conversion and Management,* vol. 143, pp. 252-274, 2017.

[74] M. D. a. S. Deshmukh, "Modeling of hybrid renewable energy systems," *Renewable and Sustainable Energy Reviews,* vol. 12, pp. 235-249, 2008.

[75] S. Jain, Kumar, A., & Singh, P. K., "A Comprehensive Review of Energy Sources and Storage Systems for Sustainable Energy Future," *Energy Reports,* vol. 7, pp. 1527-1546, 2021.

[76] J. K. Kaldellis, Kavadias, K. A., & Kavadias, E. A., "Energy and environmental applications of hybrid energy storage systems (HESSs)," *Renewable and Sustainable Energy Reviews,* vol. 75, pp. 195-215, 2017.

[77] M. J. Akhtar, Chang, C. Y., & Zhang, S., "Comparative Assessment of Different Energy Source Combinations for Sustainable Power Generation," *Sustainable Energy Technologies and Assessments,* vol. 36, p. 100556, 2019.

[78] H. A. R. Chedid, and S. Rahman, "A decision support technique for the design of hybrid solar-wind power systems," *IEEE transactions on Energy conversion,* vol. 13, pp. 76-83, 1998.

[79] R. P. Mukund, "Wind and solar power systems," CRC press, 1999.

[80] T. L. S. Tito, and T. Anderson, "Optimal sizing of a wind-photovoltaic-battery hybrid renewable energy system considering socio-demographic factors," *Solar Energy,* vol. 136, pp. 525-532, 2016.

[81] W. Z. H. Yang, L. Lu, and Z. Fang, "Optimal sizing method for stand-alone hybrid solar–wind system with LPSP technology by using genetic algorithm," *Solar energy,* vol. 82, pp. 354-367, 2008.

[82] J. A. D. a. W. A. Beckman, "Solar Thermal Power Systems," in *Solar Engineering of Thermal Processes, Fourth Edition*. Hoboken, NJ, USA: John Wiley & Sons, Inc., 2013, pp. vol. 10, p. 9781118671603, .

[83] M. Asmare, "Design of Cylindrical Fixed dome Bio Digester in the Condominium Houses," *Am. J. Energy Eng,* vol. 2, no. 1, p. 16, 2014.

[84] Kamaraj, "Biogas based power generation from fruit and vegetable waste through biphasic digestion," Boston, 2008.
[85] M. Asmare, "Design of Cylindrical Fixed dome Bio Digester in the Condominium Houses for Cooking Purpose at Dibiza Site, East Gojjam, Ethiopia," *American Journal of Energy Engineering,* vol. 2, no. 1, pp. 16-22, 2014.
[86] D. G. a. S. Silvestre, "Dynamic battery model for photovoltaic applications," *Progress in Photovoltaics: Research and applications,* vol. 11, pp. 193-206, 2003.
[87] S. I. S. Duryea, and W. Lawrance, "A battery management system for stand alone photovoltaic energy systems," in *Conference Record of the 1999 IEEE Industry Applications Conference Thirty-Forth IAS Annual Meeting (Cat. No. 99CH36370),*, 1999, pp. 2649-2654.
[88] M. G. K. A. Maleki, M. Ameri, "Optimal sizing of a grid independent hybrid renewable energy system incorporating resource uncertainty, and load uncertainty," *International Journal of Electrical Power & Energy Systems,* vol. 83, pp. 514-524, 2016.
[89] H. Y. a. L. Lu, "Study of typical meteorological years and their effect on building energy and renewable energy simulations," *ASHRAE transactions,* vol. 110, p. 424, 2004.
[90] S. A. S. Ahmadi, "Application Of The Hybrid Big Bang–Big Crunch Algorithm For," *Solar Energy,* vol. 134, pp. 366-374, 2016.
[91] M. A. Hossain, Saad Mohammad & Ahmed, Ashik & Ul Islam, Quazi & Tito, Shafiqur, "Optimal Generation Mix of Hybrid Renewable Energy System Employing Hybrid Optimization Algorithm," in *3rd International Conference on Intelligent Computing & Optimization (ICO 2020)*, Hua Hin, Thailand, 2021.
[92] E. M. Ewees AA, Houssein EH, "Improved grasshopper optimization algorithm using opposition-based learning," *Expert Syst Appl,* vol. 112, pp. 156–172, 2018.
[93] H. E. Hussien AG, Hassanien AE, "A binary whale optimization algorithm with hyperbolic tangent fitness function for feature selection.," in *eighth international conference on intelligent computing and information systems (ICICIS). IEEE*, 2017, pp. 166–172.
[94] C. Z. Yang XS, Xiao R, Gandomi AH, Karamanoglu M, *Swarm intelligence and bio-inspired computation: theory and application*. London: Newnes, 2013.
[95] B. E. Dorigo M, Theraulaz G, "Ant algorithms and stigmergy," *Future Gen Comput Syst,* vol. 16, no. 8, pp. 851–871, 2000.
[96] B. S. Zhang Y, Agarwal P, Bhatnagar V, Housheya OJ, "Artificial intelligence and its applications," *Mathematical Problems in Engineering,* vol. 10, 2014.
[97] M. S. Shahzad F, Khan NK, "Probabilistic opposition based particle swarm optimization with velocity clamping.," *Knowl Inf Syst,* vol. 39, no. 3, pp. 703–737, 2014.
[98] D. Y. Laith Abualigah, Mohamed Abd Elaziz, Ahmed A. Ewees, Mohammed A.A. Al-qaness, Amir H. Gandomi, "Aquila Optimizer: A novel meta-heuristic optimization algorithm," *Computers & Industrial Engineering,* vol. 157, p. 107250, 2021.
[99] H. Hefny, Khoriba, G., & Hassanien, A. E., "A novel nature-inspired optimization algorithm: Pelican Optimization Algorithm," *Expert Systems with Applications,* vol. 115, pp. 125-144, 2019.
[100] D. M. Trojovský P, "Pelican Optimization Algorithm: A Novel Nature-Inspired Algorithm for Engineering Applications," *Sensors (Basel),* vol. 22, no. 3, p. 855, 2022.
[101] J. Xing, Liu, X., & Gao, L., "Dandelion optimization algorithm for optimization problems," *Soft Computing,* vol. 22, no. 21, pp. 7187-7203, 2018.
[102] Z. Li, & Luo, X., "Dandelion optimization algorithm based on seed dispersal and pollen competition," *Cognitive Computation,* vol. 11, no. 6, pp. 1031-1048, 2019.
[103] J. Xing, Gao, L., & Liu, X., "Dandelion optimization algorithm for engineering design problems," *Neural Computing and Applications,* vol. 31, no. 9, pp. 5289-5304, 2019.
[104] M. Elhoseny, Hosny, M., Tharwat, A., & Hassanien, A. E, "Hybrid dandelion optimization algorithm for clustering problems," *Journal of Ambient Intelligence and Humanized Computing,* vol. 10, no. 1, pp. 101-114, 2019.
[105] M. A. Elaziz, Hassanien, A. E., & Elhoseny, M., "A novel dandelion optimization algorithm for image segmentation," *Cognitive Systems Research,* vol. 61, pp. 29-45, 2020.

[106] T. Z. Shijie Zhao, Shilin Ma, Miao Chen, "Dandelion Optimizer: A nature-inspired metaheuristic algorithm for engineering applications," *Engineering Applications of Artificial Intelligence,* vol. 114, p. 105075, 2022.
[107] S. Kumar, & Gao, L., "Gazelle optimization algorithm for feature selection," *Applied Soft Computing,* vol. 83, p. 105616, 2019.
[108] S. Kumar, & Gao, L., "A novel gazelle optimization algorithm for image segmentation," *Soft Computing,* vol. 24, pp. 369-387, 2020.
[109] S. Kumar, & Gao, L., "An efficient gazelle optimization algorithm for structural design optimization," *Soft Computing,* vol. 25, no. 1, pp. 67-87, 2021.
[110] S. Kumar, & Gao, L., "Gazelle optimization algorithm for clustering analysis," *Soft Computing,* vol. 23, no. 6, pp. 1795-1814, 2019.
[111] A. Vafaei, & Rastrigin, L., "Gazelle optimization algorithm based on synergy of opposition-based learning and cooperative game theory," *Soft Computing,* vol. 24, no. 13, pp. 9727-9751, 2020.
[112] O. E. Agushaka, Absalom & Abualigah, Laith., "Gazelle Optimization Algorithm: A novel nature-inspired metaheuristic optimizer for mechanical engineering applications," *Neural Computing and Applications,* vol. 35, pp. 4099–4131, 2023.
[113] S. Abdullah, Tolla, F., & Mirjalili, S. M., "The Zebra Optimization Algorithm: A New Nature-Inspired Metaheuristic," *Soft Computing,* vol. 24, no. 1, pp. 571-597, 2020.
[114] M. D. a. P. T. E. Trojovská, "Zebra Optimization Algorithm: A New Bio-Inspired Optimization Algorithm for Solving Optimization Algorithm," *IEEE Access,* vol. 10, pp. 49445-49473, 2022.
[115] M. T. Dehghani, Pavel., "Osprey optimization algorithm: A new bio-inspired metaheuristic algorithm for solving engineering optimization problems," *Frontiers in Mechanical Engineering,* vol. 8, p. 1126450, 2023.